Gravity as an Emergent Force Via the Uncertainty Principle

Morgan W. Weinberg

(Dated: September 7, 2026)

The core concept of this paper is the following relation between an accelerating field and time uncertainty: $a = 2c/\Delta t_u$. This relation—which derives from a hypothesized connection between the uncertainty principle and Newton's Law of Gravitation—suggests that gravity and spacetime curvature may emerge from quantum information. It's further shown that the relation is consistent with the Coulomb Force, indicating that it may be a general principle in nature. Taking this concept further, this paper draws a connection between expanding space and acceleration, which offers an explanation for the missing-mass problem in galaxies. A relationship between the expansion of space and time uncertainty is explored that allows the derivation of the mass of the observable universe.

I. NEWTON'S LAW OF GRAVITATION AND TIME UNCERTAINTY

Why Newton? Why not general relativity? Einstein's field equations reduce to the Newtonian limit for relatively low-energy gravitational systems where spacetime is essentially flat—which constitute the bulk of the observable universe. Of particular interest is the low-acceleration regime at the outer edge of rotationally-supported galaxies—where rotation curves are repeatedly found to flatten out in stark contrast to the expected Keplerian decline as seen in our Solar System. This is termed the "missing mass" problem, and the prevailing explanation for missing mass in galaxies is "dark matter", which is "dark" because it doesn't interact with light.

Here, a relation between particle acceleration, field propagation, and time uncertainty is hypothesized. In this section, the relation is investigated in the context of Newtonian gravity. In a later section, in conjunction with expanding space, the proposed relation yields a $1/r$ acceleration term that aligns with MOND (Modified Newtonian Dynamics), which is an alternative explanation for flat rotation curves that is highly predictive but not widely accepted.

$$E_f = \oint \vec{g_f} \cdot d\vec{A} = mc^2 \tag{1}$$

It is posited that a mass m has a gravitational field $\vec{g_f}$ that, when integrated over a closed surface, is equivalent to the energy contained within the surface. In the rest frame of m, the net energy of this field E_f—as shown by Eq. (1)—is independent of distance. If m is a point mass, and the closed surface is a sphere with radius r, Eq. (1) simplifies to:

$$g_f = \frac{mc^2}{4\pi r^2} \, . \tag{2}$$

It is further suggested that the field energy E_f cannot be infinitesimally divided. There is a lower bound to the elements that comprise E_f, which is found at the Planck scale. Multiplying field g_f times the Planck area a_p gives the smallest measurable unit of energy ΔE in the field at a given offset r from the point mass:

$$l_p = \sqrt{\frac{\hbar G}{c^3}} \, , \tag{3}$$

$$a_p = \pi {l_p}^2 \, , \tag{4}$$

$$a_p = \frac{hG}{2c^3} \, , \tag{5}$$

$$\Delta E = \frac{m\cancel{c^2}}{4\pi r^2}\frac{hG}{2\cancel{c^3}} \, , \tag{6}$$

$$\Delta E = \frac{mhG}{8\pi r^2 c} \, . \tag{7}$$

Eq. (3) defines the Planck length l_p [1], which, in turn, is used to define the Planck area a_p as given by Eq. (4). The definition of Planck area a_p here—with the inclusion of π as a scalar—is slightly different from that typically found in publications. With the inclusion of π, the reduced Planck constant $\hbar$ in Eq. (3) distills to its non-reduced form h in Eq. (5). If a_p is defined as a point, then ΔE represents the energy of gravitational field g_f at that point. It is imagined that particles in a gravitational field interact with the field at these points.

With ΔE defined as the smallest measurable unit of energy in a field, the time needed to measure this energy—which is to say, the time Δt_u needed for a particle to sense this energy at a point in the field—is given by the uncertainty principle:

$$\Delta E \Delta t_u \geq \frac{h}{4\pi} \, . \tag{8}$$

The time uncertainty Δt_u is deemed to be an inherent property of a gravitational field—and possibly accelerating fields in general.

Plugging Eq. (7) into Eq. (8) gives the following relations:

$$\frac{m\cancel{h}G}{8\cancel{\pi}r^2c}\Delta t_u \geq \frac{\cancel{h}}{4\cancel{\pi}} \, , \tag{9}$$

$$\frac{mG}{2r^2c}\Delta t_u = 1 \, . \tag{10}$$

Notice that as Eq. (9) progresses to Eq. (10), the $\geq$ sign has been replaced with an equals sign. This will pin Δt_u to its minimal value—with the understanding that ΔE

has also been defined as a minimum.

Particles, in general, transfer information via fields. It's hypothesized that there is uncertainty in this information and that this uncertainty—coupled with the rate of information flow—results in acceleration relative to the field.

It's well established that information travels at c for all observers. This is embodied by Eq. (11) where Δt_f is the time it takes for the field to travel a distance of Δr:

$$\frac{\Delta r}{\Delta t_f} = c \; . \tag{11}$$

Multiplying Eq. (10) by Eq. (11) gives this:

$$\frac{mG}{2r^2 \cancel{c}} \Delta t_u \cancel{c} = \frac{\Delta r}{\Delta t_f} \; , \tag{12}$$

$$\frac{mG}{2r^2} = \frac{\Delta r}{\Delta t_f \Delta t_u} \; . \tag{13}$$

Essentially, Eq. (13) relates a field that conveys information to a point in the field where that information in sensed—where, at that point, there is uncertainty in the information. Here, it's imagined that there is a field surrounding mass m and that field contains information that describes the energy contained within in it. The uncertainty in that information—as measured by Δt_u—increases according to the inverse square of distance, which is to say, the information density of the field decreases with respect to surface area. Δr and Δt_f, in Eq. (13), describe the rate at which this information is transfered, where Δr is a radial distance in the direction of information flow, which is outward from mass m.

Non-relativistic acceleration is described by the familiar equation:

$$\Delta r = \frac{1}{2} a {\Delta t_p}^2 \; , \tag{14}$$

$$ {\Delta t_p}^2 = \frac{2\Delta r}{a} \; . \tag{15}$$

The right side of Eq. (13) has the units of acceleration, and this combination of terms encapsulates the hypothesis that uncertainty in a flow information results in acceleration relative to that flow. With Δr established as a *radial* distance, Eq. (15) is plugged into Eq. (13), which reduces to Newton's equation for gravity:

$$\frac{mG}{\cancel{2}r^2} = \frac{\cancel{\Delta r} a}{\cancel{2}\cancel{\Delta r}} \; , \tag{16}$$

$$a = \frac{mG}{r^2} \; . \tag{17}$$

Notice that in Eq. (13), $\Delta t_f \Delta t_u$ has been substituted with ${\Delta t_p}^2$, which is asserting an equivalence that clearly needs to be unpacked.

Fig. 1 shows a particle accelerating leftward through a minute distance Δr from one point in space to another. The points may be considered as points in a field, where information is propagating from the left point to the right point at c. A particle in the field at the right point, sensing that information, which has uncertainty—as measured by time uncertainty of Δt_u—is accelerated opposite the direction of information flow as follows:

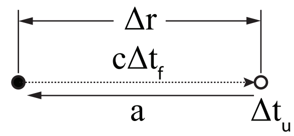

FIG. 1. Acceleration between discreet points in a field.

$$\Delta t_f = \frac{\Delta r}{c} \; ,$$

$$ {\Delta t_p}^2 = \frac{2\Delta r}{a} \; ,$$

$$ {\Delta t_p}^2 = \Delta t_f \Delta t_u \; , \tag{18}$$

$$\frac{2\cancel{\Delta r}}{a} = \frac{\cancel{\Delta r}}{c} \Delta t_u \; , \tag{19}$$

$$a = \frac{2c}{\Delta t_u} \; . \tag{20}$$

Eq. (15) relates ${\Delta t_p}^2$ to acceleration, which, along with Eq. (11) allow the Δr terms to cancel, leaving Eqs. (20).

Applying direction to the magnitudes of acceleration and field speed—as shown in Fig. 1—gives the vector form of Eq. (20):

$$\vec{a} = -\frac{2\vec{c}}{\Delta t_u} \; . \tag{21}$$

In Eq. (21), Δt_u is a property of the field, and $\vec{c}$ is the field's propagation velocity relative to the point in the field where Δt_u is measured. $\vec{a}$ gives the exact acceleration of a particle that is initially at rest in the field but is sufficiently accurate for particles with non-relativistic speeds. Clearly, Eq. (21) has a large numerator. Plugging Earth's near-surface gravity acceleration of 9.81 m s^{-2} into this equation gives a time uncertainty of 1.94 years.

Importantly, the claim in this section is not that Newton's equation for gravity is derived via the uncertainty principle, but that uncertainty relates to acceleration, which relates to gravity. To recap, Eq. (13) derives from the following thesis: There is a gravitational field surrounding a mass such that Gauss' integral of the field equates to the rest energy of the mass. The field is measured at points that are defined by the Plank area. Because of the scale of measurement, the uncertainty principle must come into play. The field can be imagined as the means by which information flows from the mass to surrounding particles. It's also understood that information travels at c. Combining these concepts gives Eq. (13), which looks very similar to Newton's equation for gravity—with the right side having units of accel-

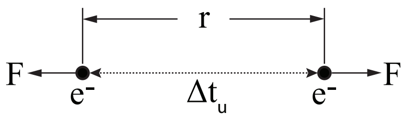

FIG. 2.

eration. Interestingly, the gravitational constant G in Eq. (13) was never purposely introduced but comes from the Plank area. It is the last constant standing from this definition.

Eqs. (18)–(21) are needed as a bridge between Eq. (13) and Eq. (17), which is Newton's equation for gravity. Hence, Eq. (21) is partially derived *from* Newton's equation. As somewhat of a tautology, Eq. (21) is also asserted to be the source of gravitational acceleration.

II. COULOMB FORCE

Fig. 2 shows two electrons separated by a distance r. As a quick sanity check of Eq. (21), this equation is applied to the virtual-photon description of electromagnetic interaction to see if it reproduces the Coulomb force between these electrons.

A virtual photon emitted between the electrons would have an energy given by the uncertainty principle:

$$\Delta E \Delta t \geq \frac{\hbar}{2} ,$$
$$\Delta E \geq \frac{\hbar}{2\Delta t} . \qquad (22)$$

ΔE can be expressed as an equivalent mass m_e as follows:

$$m_e = \frac{\Delta E}{c^2} ,$$
$$m_e = \frac{\hbar}{2c^2\Delta t} . \qquad (23)$$

Because ΔE is a minimum, the $\geq$ sign in Eq. (22) can be replaced with an equals sign. With the application of Eq. (21), the reactive force on an electron emitting the virtual photon is thus:

$$F_p = ma ,$$
$$F_p = m_e \frac{2c}{\Delta t_u} ,$$
$$F_p = \frac{\hbar}{\cancel{2}c^{\cancel{2}}\Delta t}\frac{\cancel{2}\cancel{c}}{\Delta t_u} . \qquad (24)$$

The lifespan Δt and the uncertainty Δt_u of the virtual photon are equivalent. Both equate to r/c. Plugging this result into Eq. (24) gives the following:

$$F_p = \frac{\hbar}{c\Delta t \Delta t_u} ,$$
$$F_p = \frac{\hbar c^{\cancel{2}}}{\cancel{c}r^2} ,$$
$$F_p = \frac{\hbar c}{r^2} . \qquad (25)$$

Eq. (25) gives the reactive force F_p on an electron from the emission of a virtual photon. To translate this reactive force to the Coulomb force between the electrons, F_p is multiplied by the Sommerfeld constant α. This constant relates the potential energy PE_c between two electrons at a distance r and the energy E_p of a photon of angular wavelength r where:

$$\alpha E_p = PE_c ,$$
$$\alpha \frac{\partial E_p}{\partial r} = \frac{\partial PE_c}{\partial r} ,$$
$$\alpha = \frac{F_c}{F_p} .$$

Taking the partial derivative of these energies with respect to r gives a relation between the Coulomb force and the force of a photon of energy E_p. With this relation, the Coulomb force is given by multiplying Eq. (25) by α—the latter defined below:

$$\alpha = \frac{e^2}{4\pi\epsilon_0\hbar c} ,$$
$$F_c = \alpha\frac{\hbar c}{r^2} ,$$
$$F_c = \frac{e^2\cancel{\hbar c}}{4\pi\epsilon_0\cancel{\hbar c}r^2} ,$$
$$F_c = \frac{e^2}{4\pi\epsilon_0 r^2} . \qquad (26)$$

Eq. (26) is the familiar equation for the Coulomb force, where e is the charge of an electron and r is the distance between charges. While the details of the virtual-particle exchange mechanism—as described by QFT (quantum field theory)—are significantly more complicated, the aim of this exercise was to serve as a quick sanity check of Eq. (21) in a context other than gravity.

1. *The Application of Eq. (21)*

In the rest frame of an electron, a virtual photon with time uncertainty Δt_u and velocity c is emitted by the electron. With Eq. (21), an electron, at the time of emission, is accelerated by a—opposite in direction to the flow of information towards the second electron. Here, information is conveyed by a virtual photon.

This raises a question: In a gravitational field, is the acceleration of a particle more precisely a consequence of fluctuations in the field? In other words, in the context

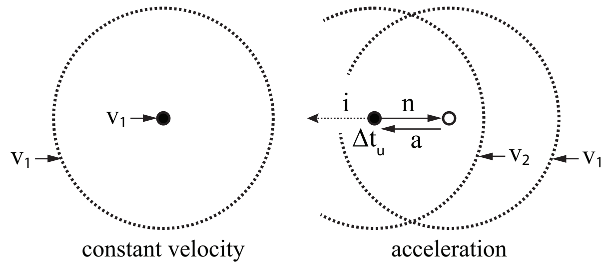

FIG. 3.

of gravity, does Δt_u, in Eq. (21), refer to the lifespan of a virtual graviton?

In a weak-field quantum description of gravity, the graviton would be a massless spin-2 field quantum that couples to the stress-energy tensor. In QFT, the exchange of an even-spin virtual particle (spin-0 scalars or spin-2 gravitons) produces a purely attractive force, which aligns with our observations of gravity. For electromagnetism, the force is mediated by the photon, a massless spin-1 gauge boson that couples to the electromagnetic four-current [4].

III. INERTIA

If Eq. (21) can describe acceleration from an external field, can it also elucidate the mystery of inertia?

Imagine two capsules in space, separated by a certain distance, at rest with respect to each other. The second capsule fires its engine and starts accelerating. From the vantage point of an observer in the second capsule, the first capsule looks to be moving, and its relative velocity seems to be increasing. Conversely, an observer in the first capsule sees the second capsule moving at an increasing velocity. From the perspective of either observer, the other is accelerating.

There is, however, additional information that these observers can use to determine who, in fact, is accelerating. The second observer, looking at the accelerometers in the cabin, could measure his rate of acceleration. The second observer—assuming that he was facing the direction of acceleration—would be pressed into his seat, which would be pushing against the inertia of his body. The first observer, looking at his instruments, would detect no such acceleration—remaining essentially weightless in his seat. Here, inertia is the source of truth. It informs which observer is *actually* accelerating.

At a certain point, the second observer looks out of his window and sees the first capsule moving at a velocity v_1. Assuming that the first capsule and its gravitational field are at rest with respect to each other, the second observer would see the first capsule *and its field* moving at v_1—as illustrated by the left diagram in Fig. 3. As the relative velocity increases, the first capsule and its field, which continue to remain at rest with respect to each other—from the perspective of the second observer, move in concert.

Does this hold in the opposite perspective—where the first observer is looking at the second capsule? If the engine of the second capsule were to be cut off, and it stopped accelerating, the capsule wouldn't have detached from its field. The second capsule and its field would be at rest with respect to each other. Therefore, even during acceleration, the second capsule's field must be accelerating along with the capsule.

It's posited that accelerating this field requires information flow—which, in effect, is how the second observer comes to realize that *he* is the one who is accelerating. Looking at Eq. (21), if this equation is run in reverse, acceleration coupled with time uncertainty—which is related to the measurable energy at a point in the field—can drive information flow in the field. Here, the acceleration of particles of and within the second capsule is informing the fields around those particles. Further, it's surmised that the inertia—the resistance to acceleration—experienced by the second observer as he is pressed into his seat is a result of that observer interacting with his *own* gravitational field. This interaction, during acceleration, is continuously re-informing his field.

In short, if gravity can be described as information flow driving acceleration, inertia can be thought of as acceleration driving information flow. Here, inertia is the price of re-informing the field around an accelerating mass. Note that Eq. (21) has no mass terms, and implicitly makes no distinction between gravitational mass and inertial mass. Further, there's no distinction between gravitational information flow and inertial information flow. Thus, it's imagined that Eq. (21) is compatible with the weak equivalence principle.

The right diagram in Fig. 3 shows a particle of the second capsule accelerating its own field from v_1 to v_2. Acceleration $\vec{a}$ drives information flow $\vec{i}$ leftward into the field—in the direction of acceleration. This information flow, as measured by Δt_u, is such that the inertial acceleration—represented by $\vec{n}$ in the diagram—is equal and opposite to the applied acceleration $\vec{a}$. As described by Eq. (21), the direction of $\vec{n}$ is opposite to that of information flow $\vec{i}$.

Δt_u, in this case, is not fine tuned. It's precisely what this parameter would evaluate to with $\vec{a}$ plugged into Eq. (21)—with the negative sign in the equation ignored. While seemingly a tautology, if acceleration drives information flow, it's logical that the same information flow would result in counter-acceleration of equal magnitude.

Also notice that time uncertainty in Eq. (21) is inversely proportional to acceleration, which means that as acceleration approaches infinity, time uncertainty approaches zero. Perhaps time uncertainty, here, can be thought of as the urgency with which information must flow, where higher rates of acceleration require higher rates of information transfer. As acceleration goes to zero, time uncertainty goes to infinity, indicating that information flow is no longer necessary.

IV. A GRAVITATIONAL FIELD IN EXPANDING SPACE

If photons are redshifted over time by expanding space as they propagate, can gravitational fields also be redshifted as they propagate? Are all propagating fields in expanding space subject to redshift? With respect to photons, cosmological redshift is literally the shifting of a photon's frequency to the red end of the spectrum as a consequence of its wavelength being stretched by expanding space. An observer of a redshifted photon will have noticed its energy having been decreased relative to its emitted frequency.

Gravitational fields, however, show no signs of dilution over time—with gravitational systems remaining stable over billions of years. Even at the outermost edges of galaxies, thousands of light-years from their centers (that comprise the bulk of the galactic mass), there is no indication of a weakening field. In fact, the opposite is true; this field typically seems to have more strength than the mass of the galaxy can account for—as evidenced by flat rotation curves.

This is actually a clue. Unlike light, a gravitational field is intrinsically connected to its source. As the source translates or accelerates, the field must move in concert. If the source loses or gains energy, the field strength changes in proportion thereto. In short, the field requires a constant flow of information to maintain its connection with its source. With this in mind, it may be more correct to imagine a gravitational field in expanding space as continuously being stretched and re-informed, with the latter immediately undoing any dilution.

Eq. (7), restated below, gives the energy uncertainty at a point in a field. Taking the derivative with respect to time gives the following:

$$\Delta E = \frac{mhG}{8\pi r^2 c} \ ,$$
$$\frac{d\Delta E}{dt} = \frac{-mhG}{4\pi r^3 c}\frac{dr}{dt} \ . \tag{27}$$

The expansion of space is given by:

$$\vec{v} = \vec{r}H_l \ , \tag{28}$$
$$\frac{dr}{dt} = rH_l \ . \tag{29}$$

Eq. (28) is recognizable as Hubble's law, which is usually written with the Hubble parameter H_0—a measure of intergalactic expansion. Notice that Eqs. (28) and (29) use the parameter H_l, which is proffered as a local measure of expansion (or "expansion parameter") at a specific point in a frame of reference. The case for the idea—that the expansion parameter measured by an observer is dependent on that observer's frame of reference—will be built slowly over the course of the following sections. This will, hopefully, lead to a reconciliation of H_l and H_0.

Plugging Eq. (29) into Eq. (27) gives the following:

$$\frac{d\Delta E}{dt} = \frac{-mhG}{4\pi r^{\cancel{3}2} c}\cancel{r}H_l \ , \tag{30}$$
$$\frac{\Delta(\Delta E)}{\Delta t_u} = \frac{-mhGH_l}{4\pi r^2 c} \ , \tag{31}$$
$$\Delta E = \frac{mhGH_l}{4\pi r^2 c}\Delta t_u \ . \tag{32}$$

There's a lot going on between Eq. (30) and Eq. (32) that needs to be deconstructed. Eq. (30) shows the energy at a point in a gravitational field that is decreasing over time as a result of being stretched in expanding space. In Eq. (31), $d(\Delta E)$ and dt are quantized to $\Delta(\Delta E)$ and Δt_u, with the presumption that any change in energy, at this scale, would be discrete over a finite period of time. In Eq. (32), $\Delta(\Delta E)$ is simplified to ΔE with the observation that the latter *is* the change in energy in question.

Also, notice that the negative sign has been stripped from the definition of ΔE. As discussed, the strength of this field, being a function of the source mass, does not dilute over time. If a mass is stable, its field must remain stable in concert. This means that a negative ΔE must be balanced with a positive ΔE as the field is re-informed. The ΔEs cancel, which means there is no net energy transfer to or from the field as a consequence of expanding space.

Plugging Eq. (32) into the uncertainty equation (Eq. (8)) gives the following:

$$\Delta E \Delta t_u = \frac{h}{4\pi} \ ,$$
$$\frac{m\cancel{h}GH_l}{\cancel{4\pi}r^2 c}{\Delta t_u}^2 = \frac{\cancel{h}}{\cancel{4\pi}} \ , \tag{33}$$
$$\Delta t_u = \frac{r\sqrt{c}}{\sqrt{mGH_l}} \ . \tag{34}$$

As before, with ΔE and Δt_u defined as minima, the $\geq$ sign in the uncertainty equation has been replaced with an equals sign. Note that the time uncertainty Δt_u in Eq. (32) corresponds to Δt_u in Eq. (8), as they are both measuring the same energy. This is reflected in the ${\Delta t_u}^2$ term of Eq. (33). Solving for Δt_u gives Eq. (34)—a relation between time uncertainty Δt_u and local-frame expansion H_l.

Eq. (20) may then be used to convert this time uncertainty to acceleration:

$$a = \frac{2c}{\Delta t_u} \ ,$$
$$a = \frac{2c\sqrt{mGH_l}}{r\sqrt{c}} \ , \tag{35}$$
$$a = \frac{2\sqrt{cH_l mG}}{r} \ . \tag{36}$$

The acceleration term defined by Eq. (36) is designated as the non-Newtonian or "expansion" component and is additive to the Newtonian term given by Eq. (17). Because the direction of field propagation is the same for both components, both accelerations point toward the field source. Combining these terms gives a complete equation for acceleration in the Newtonian limit:

$$a_n = \frac{mG}{r^2} + \frac{2\sqrt{cH_l mG}}{r} \; . \tag{37}$$

V. THE RELATION TO MOND

In Section VI, a more general form of Eq. (37) will be derived in the context of a system of particles. Before moving on, however, the similarity between Eq. (36) and the deep-MOND equation for acceleration should be discussed.

MOND (Modified Newtonian Dynamics), proposed by Mordehai Milgrom in 1983 [5] [6] [7], offers an alternative to dark matter as an explanation for the flattening of galactic rotation curves. MOND is an algorithm that separates regimes of acceleration according to an empirically derived constant a_0. Gravitational accelerations far above a_0 remain Newtonian, whereas accelerations far below a_0, termed the “deep-MOND regime”, taper to the following relation:

$$a = \frac{\sqrt{a_0 mG}}{r} \; . \tag{38}$$

An interpolation function mathematically bridges the Newtonian and deep-MOND regimes. Milgrom’s initial estimate of a_0 was slightly higher than the accepted value of 1.2E−10 m s^{-2}, originally estimated by Begeman et al. in 1991 [8]. Interestingly, a_0 has not materially wavered from this value in the ensuing decades since the early 1990s, even as the catalog of galaxies with measurable rotation curves has vastly expanded.

Note the congruence between Eqs. (38) and (36), with both having an acceleration $a \propto \sqrt{mG}/r$. Both of these equations satisfy the Baryonic Tully-Fisher Relation (BTFR), which holds that $v^4 \propto m$ [9] [10] [11]:

$$\begin{aligned} \frac{v^2}{\cancel{r}} &= a = \frac{\sqrt{a_0 mG}}{\cancel{r}} \; , \\ v^4 &= a_0 mG \; . \end{aligned} \tag{39}$$

In this relation, v is the speed of a particle in circular orbit around a galaxy of mass m—at the outer edge where the Newtonian component is a small fraction of the net acceleration. The rotation curve, given by this relation, mathematically flattens out—as speed is independent of distance.

Three predictions stem from MOND: The rotation curves of isolated galaxies flatten out. The speed at the flat end of rotation curves raised to the power of four is proportional to the galaxy mass, and the constant a_0 marks the transition to the non-Newtonian acceleration regime. These are specific predictions that leave MOND and the BTFR very exposed to falsification. Extensive galaxy surveys, however, repeatedly find MOND to be consistent with observations, and this holds for low-mass and high-mass galaxies with varying levels of surface brightness [12] [13] [14] [15] [16].

Another confirmation of the flatness prediction comes from a recent paper where the authors used weak-gravitational-lensing data from the KiDS survey to construct the extended rotation curves of isolated galaxies [17], which appear to remain flat even out to 1 Mpc with no sign of decline!

Put succinctly, “If the universe is made of cold dark matter, why does MOND get any predictions right?” [18] It seems highly unlikely that the predictive successes of MOND are mere coincidences, but rather an admonition that our understanding of gravity in the low-acceleration regime is likely incomplete. In this respect, the BTFR and MOND serve as salient guidestones along the path to a more complete comprehension of nature—on par with Kepler’s discovery that the planets have elliptical orbits.

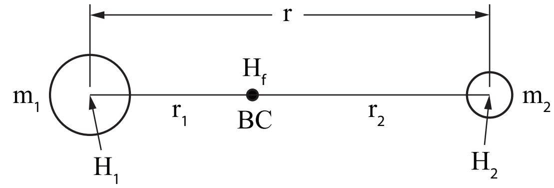

FIG. 4.

VI. TWO-BODY SYSTEM

Fig. 4 shows a two-body system with masses m_1 and m_2, separated by distance r, with barycenter BC; and where m_1 is of larger mass than m_2. With Eq. (37), the attractive force between the two masses is thus:

$$F_1 = m_1 \left(\frac{m_2 G}{r^2} + \frac{2\sqrt{cH_2 m_2 G}}{r} \right) \; , \tag{40}$$

$$F_2 = m_2 \left(\frac{m_1 G}{r^2} + \frac{2\sqrt{cH_1 m_1 G}}{r} \right) \; , \tag{41}$$

$$F_1 = F_2 \; . \tag{42}$$

F_1 is the magnitude of the force on m_1 by m_2’s gravitational field, and vice versa for F_2. In the Newtonian limit considered here, F_1 and F_2 must be equal and opposite according to Newton’s Third Law of Motion—which is to say, the momentum of the system must be conserved.

H_2, in Eq. (40), refers to the local expansion parameter at m_2; and conversely, H_1, in Eq. (41), refers to the local expansion parameter at m_1. For F_1 to be equivalent to F_2, H_1 and H_2 must differ, which will shortly be clear.

Here, it’s posited that the frame of reference comprising the m_1–m_2 system has an expansion parameter H_f, where H_1 and H_2 are linear functions of H_f as follows:

$$H_1 = k_1 H_f \ , \tag{43}$$
$$H_2 = k_2 H_f \ , \tag{44}$$

where k_1 and k_2 are constants.

With these relations, equating F_1 and F_2, gives the following:

$$\begin{aligned}
& m_1 \left(\frac{m_2 G}{r^2} + \frac{2\sqrt{ck_2 H_f m_2 G}}{r} \right) = \\
& \qquad m_2 \left(\frac{m_1 G}{r^2} + \frac{2\sqrt{ck_1 H_f m_1 G}}{r} \right) \ , \\
& \cancel{\frac{m_1 m_2 G}{r^2}} + \frac{2m_1\sqrt{ck_2 H_f m_2 G}}{r} = \\
& \qquad \cancel{\frac{m_2 m_1 G}{r^2}} + \frac{2m_2\sqrt{ck_1 H_f m_1 G}}{r} \ ,
\end{aligned}$$

which, in turn, reduces to:

$$\begin{aligned}
& \frac{\cancel{2} m_1\sqrt{\cancel{c} k_2 \cancel{H_f} m_2 \cancel{G}}}{\cancel{r}} = \frac{\cancel{2} m_2\sqrt{\cancel{c} k_1 \cancel{H_f} m_1 \cancel{G}}}{\cancel{r}} \ , \\
& m_1\sqrt{k_2 m_2} = m_2\sqrt{k_1 m_1} \ , \\
& \sqrt{m_1 k_2} = \sqrt{m_2 k_1} \ , \\
& \frac{k_1}{k_2} = \frac{m_1}{m_2} \ . \qquad (45)
\end{aligned}$$

Taking the ratio of Eqs. (43) and (44) and plugging Eq. (45) into the result, yields this:

$$\frac{H_1}{H_2} = \frac{m_1 H_f}{m_2 H_f} \ , \tag{46}$$
$$H_1 = k m_1 H_f \ , \tag{47}$$
$$H_2 = k m_2 H_f \ . \tag{48}$$

Eqs. (47) and (48) show that the expansion parameter at each mass is proportional to that mass. In separating these two equations from Eq. (46), a new constant k is introduced—noting that the ks would cancel upon retaking the ratio of H_1 and H_2. Adding Eqs. (47) and (48) together gives this:

$$H_1 + H_2 = k(m_1 + m_2) H_f \ . \tag{49}$$

If the sum of the local expansion parameters in the frame is set equal to the expansion parameter of the frame H_f, Eq. (49) can be solved for k:

$$H_1 + H_2 = H_f \ , \tag{50}$$
$$1 = k(m_1 + m_2) \ , \tag{51}$$
$$k = \frac{1}{m_1 + m_2} \ . \tag{52}$$

The correctness of Eq. (50) will become more evident as the discussion continues. With this relation for k, Eqs. (47) and (48) can be rewritten as functions of the frame's expansion parameter H_f and the masses in that frame:

$$H_1 = \frac{m_1}{m_1 + m_2} H_f \ , \tag{53}$$
$$H_2 = \frac{m_2}{m_1 + m_2} H_f \ . \tag{54}$$

What these relations are revealing is that the masses in a system govern the rates of expansion seen by the particles in that system. The expansion rate, however, given by Eq. (28)—which underpins the acceleration and force equations that follow—has no mass terms and is a function of distance! The next step is to reconcile Eqs. (53) and (54) with Eq. (28).

In Fig. 4, distances r_1 and r_2 are related to m_1 and m_2 as follows:

$$\frac{r_1}{r_2} = \frac{m_2}{m_1} \ . \tag{55}$$

This ratio holds regardless of the motions of these masses. Whether they are in circular orbits, eccentric orbits, or accelerating toward each other in a straight line, the barycenter of m_1 and m_2 maintains the ratio given by Eq. (55). Versions of this equation with r in the denominator of the distance ratio are deduced as follows:

$$\begin{aligned}
& \frac{r_1}{r_2} + 1 = \frac{m_2}{m_1} + 1 \ , \\
& \frac{r_1}{r_2} + \frac{r_2}{r_2} = \frac{m_2}{m_1} + \frac{m_1}{m_1} \ , \\
& \frac{r_1 + r_2}{r_2} = \frac{m_1 + m_2}{m_1} \ , \\
& \frac{r_2}{r} = \frac{m_1}{m_1 + m_2} \ , \qquad (56) \\
& \frac{r_1}{r} = \frac{m_2}{m_1 + m_2} \ . \qquad (57)
\end{aligned}$$

Applying Eq. (28) to the two-body system of Fig. 4, gives the expansion rates at m_1 and m_2:

$$v_1 = r H_2 \ , \tag{58}$$
$$v_2 = r H_1 \ . \tag{59}$$

With m_2 as an origin, space expanding from this point has an expansion rate of v_1 as measured at m_1. This is embodied by Eq. (58). Likewise, Eq. (59) gives the expansion rate v_2 relative to m_1—as seen by m_2.

Here, it's postulated that the expansion rate v_1 measured at m_1 should be consistent at a given point in time, regardless of the chosen origin along the line of expansion. This would likewise hold for v_2 as measured at m_2. In other words, **the expansion rate measured at a point in a reference frame—in a particular direction at a point in time—should be invariant with respect to an arbitrary origin of expansion along the line of measurement**.

Further, referring back to Eq. (27), the idea—that dr/dt (v_1 and v_2 in the present example) relative to a reference mass should be consistent—is required by this equation, which relates a physical effect $d\Delta E/dt$ to an expansion rate dr/dt. It doesn't make sense that this physical effect should change as a result of choosing different coordinates.

Thus, with the barycenter set as the origin of expansion, the following relations can be written:

$$v_1 = r_1 H_f \ , \tag{60}$$
$$v_2 = r_2 H_f \ . \tag{61}$$

Notice that Eqs. (60) and (61) are functions of H_f, the expansion parameter at the barycenter, which is the same origin for both observers m_1 and m_2. Contrast this with the case above for Eqs. (58) and (59), where the observers see expansion rates from different perspectives and origins.

Equating Eqs. (58) and (59) with Eqs. (60) and (61) distills as follows:

$$rH_2 = r_1 H_f \ , \tag{62}$$
$$rH_1 = r_2 H_f \ , \tag{63}$$
$$H_1 = \frac{r_2}{r} H_f \ , \tag{64}$$
$$H_2 = \frac{r_1}{r} H_f \ , \tag{65}$$
$$H_1 = \frac{r_2}{r_1} H_2 \ . \tag{66}$$

Plugging Eqs. (56) and (57) into Eqs. (64) and (65), recovers Eqs. (53) and (54):

$$H_1 = \frac{m_1}{m_1 + m_2} H_f \ , \tag{67}$$
$$H_2 = \frac{m_2}{m_1 + m_2} H_f \ . \tag{68}$$

Thus, given a two-body system of masses m_1 and m_2, with a frame of reference at the barycenter—with the frame having an expansion parameter of H_f, Eqs. (53) and (54) give the local expansion parameters at m_1 and m_2, respectively. As demonstrated, these local expansion parameters are functions of barycenter distances, which in turn are functions of mass. Importantly, these relations allow the force vectors—on m_1 by m_2 and conversely, on m_2 by m_1—to cancel, avoiding a possible inconsistency.

Here, the above equations for a two-body system are generalized for an n-body system. Evidence to support this extrapolation will be built in the following sections. The general form of Eqs. (53) and (54) is thus:

$$H_r = \frac{m_r}{m_t} H_f \ . \tag{69}$$

Eq. (69) relates the expansion parameter H_r at the barycenter of a reference mass m_r (or collection of masses) to that of another mass or collection of masses m_t, where H_f is the expansion parameter at the barycenter of m_t. m_t may include m_r, in which case H_f is the expansion parameter at the barycenter of the entire system.

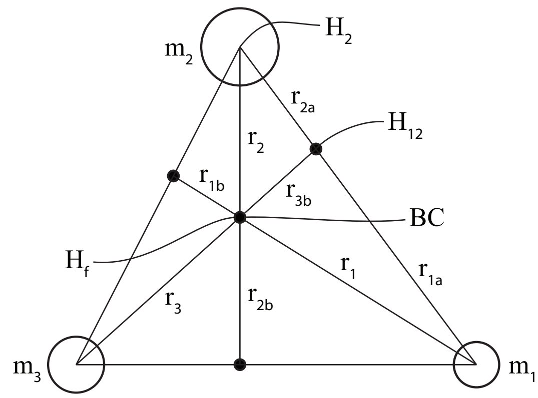

FIG. 5.

With Eqs. (37) and (69), a general relation for the magnitude of acceleration relative to a reference mass m_r, in an n-body system of total mass m_t, is as follows:

$$a_n = \frac{m_r G}{r^2} + \frac{2\sqrt{cH_r m_r G}}{r} \ ,$$
$$a_n = \frac{m_r G}{r^2} + \frac{2m_r\sqrt{cH_f G}}{r\sqrt{m_t}} \ ,$$
$$a_n = \frac{m_r G}{r}\left(\frac{1}{r} + \frac{2\sqrt{cH_f}}{\sqrt{m_t G}}\right) \ . \tag{70}$$

With the arguments surrounding Eqs. (60)–(66), Eq. (50) is assumed to have been correct. Extending this relation to the general case gives this:

$$H_f = \sum_{i=1}^{n} H_i \ . \tag{71}$$

Eq. (71) shows that in a system of n bodies with an expansion parameter of H_f at the barycenter, the sum of local expansion parameters for these bodies is equivalent to H_f.

VII. THREE-BODY SYSTEM

As a quick sanity check of the n-body-system equations, the concepts from the last section are applied to a three-body system and checked for consistency. Fig. 5 shows a three-body system of dissimilar masses. The center dot in the triangle marks the barycenter BC of the system, and the dots on the edges denote the centers of mass of the two bodies along each edge. The relations between distances and masses in this figure can be written as follows:

$$\frac{r_3}{r_{3b}} = \frac{m_1 + m_2}{m_3} \ , \tag{72}$$

$$r_{3c} = r_3 + r_{3b} \ , \tag{73}$$

$$r_{3c} = \left(\frac{m_1 + m_2}{m_3}\right) r_{3b} + r_{3b} \ , \tag{74}$$

$$r_{3c} = \left(\frac{m_1 + m_2}{m_3} + \frac{m_3}{m_3}\right) r_{3b} \ , \tag{75}$$

$$\frac{r_{3b}}{r_{3c}} = \frac{m_3}{m_1 + m_2 + m_3} \ , \tag{76}$$

$$\frac{r_3}{r_{3c}} = \frac{m_1 + m_2}{m_1 + m_2 + m_3} \ . \tag{77}$$

Equating rates of expansion at m_3 along the line extending from H_{12} gives this:

$$v_3 = (r_3 + r_{3b}) H_{12} \ , \tag{78}$$

$$v_3 = r_3 H_f \ , \tag{79}$$

$$H_{12} = \frac{r_3}{r_3 + r_{3b}} H_f \ . \tag{80}$$

Plugging Eq. (77) into Eq. (80) yields this:

$$H_{12} = \frac{m_1 + m_2}{m_1 + m_2 + m_3} H_f \ . \tag{81}$$

With H_{12} marking the barycenter of m_1 and m_2, distance is related to mass as follows:

$$\frac{r_{1a}}{r_{2a}} = \frac{m_2}{m_1} \ , \tag{82}$$

$$\frac{r_{1a}}{r_{1a} + r_{2a}} = \frac{m_2}{m_1 + m_2} \ . \tag{83}$$

With a definition for H_{12}, the expansion parameter at m_2 can also be determined via the expansion rate at m_1:

$$v_1 = (r_{1a} + r_{2a}) H_2 \ , \tag{84}$$

$$v_1 = r_{1a} H_{12} \ , \tag{85}$$

$$H_2 = \frac{r_{1a}}{r_{1a} + r_{2a}} H_{12} \ . \tag{86}$$

Plugging Eqs. (81) and (83) into Eq. (86) is thus:

$$H_2 = \frac{m_2}{\cancel{m_1 + m_2}} \frac{\cancel{m_1 + m_2}}{m_1 + m_2 + m_3} H_f \ ,$$

$$H_2 = \frac{m_2}{m_1 + m_2 + m_3} H_f \ . \tag{87}$$

Note the congruency between this equation and the general local-expansion relation given by Eq. (69), where H_2 is the expansion parameter at reference mass m_2. With Eq. (69) satisfied, agreement with Eq. (70) follows when

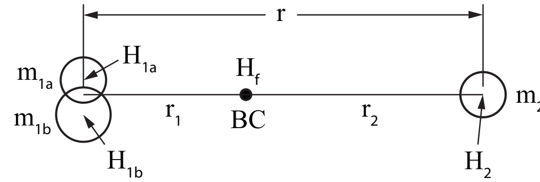

FIG. 6.

H_2 is plugged into Eq. (37):

$$m_t = m_1 + m_2 + m_3 \ ,$$

$$H_r = \frac{m_2}{m_t} H_f \ ,$$

$$a_n = \frac{m_2 G}{r^2} + \frac{2\sqrt{c m_2 H_f m_2 G}}{r\sqrt{m_t}} \ ,$$

$$a_n = \frac{m_2 G}{r} \left(\frac{1}{r} + \frac{2\sqrt{c H_f}}{\sqrt{m_t G}}\right) \ .$$

Agreement with Eq. (71) is also observed upon taking the sum of the expansion parameters at the three masses. Note, the relations H_1 and H_3 below are readily derived with the same approach used for H_2:

$$H_1 = \frac{m_1}{m_t} H_f \ ,$$

$$H_2 = \frac{m_2}{m_t} H_f \ ,$$

$$H_3 = \frac{m_3}{m_t} H_f \ ,$$

$$H_1 + H_2 + H_3 = \frac{\cancel{m_t}}{\cancel{m_t}} H_f = H_f \ .$$

Here, the above n-body relations are recovered.

VIII. SPLIT TWO-BODY SYSTEM

Fig. 6 has the same two-body system of Fig. 4 with mass m_1 having been split into two unequal parts, m_{1a} and m_{1b}. In the figure, visually, the two parts are slightly offset. Mathematically, however, assume they are coincident. Using Eq. (70), the magnitude of the forces between m_{1a}, m_{1b}, and m_2 is thus:

$$m_t = m_{1a} + m_{1b} + m_2 \ ,$$

$$F_{1a2} = \frac{m_{1a} m_2 G}{r} \left(\frac{1}{r} + \frac{2\sqrt{c H_f}}{\sqrt{m_t G}}\right) \ ,$$

$$F_{1b2} = \frac{m_{1b} m_2 G}{r} \left(\frac{1}{r} + \frac{2\sqrt{c H_f}}{\sqrt{m_t G}}\right) \ ,$$

$$F_{12} = \frac{(m_{1a} + m_{1b}) m_2 G}{r} \left(\frac{1}{r} + \frac{2\sqrt{c H_f}}{\sqrt{m_t G}}\right) \ .$$

Looking at the above equations, the individual force on an element of m_1 is proportional to its mass, and the sum

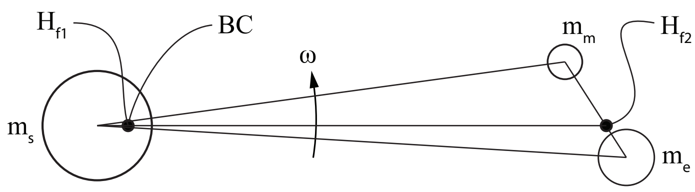

FIG. 7.

of those forces equates to the net force F_{12} between m_1 and m_2, as consistency would demand.

IX. RESTRICTED THREE-BODY SYSTEM

Fig. 7 shows a restricted three-body system with an isolated two-body system orbiting a relatively large mass. This is the relationship between the Earth, Moon, and the Sun. The force between the Earth and the Moon, as calculated in the three-body reference frame, which has an expansion parameter of H_{f1} at the Sun–Earth–Moon barycenter, is thus:

$$F_{em} = \frac{m_e m_m G}{r}\left(\frac{1}{r} + \frac{2\sqrt{cH_{f1}}}{\sqrt{(m_s + m_e + m_m)G}}\right) . \tag{88}$$

In the Earth–Moon reference frame, with an expansion parameter of H_{f2}, the force between the Earth and the Moon is this:

$$F_{em} = \frac{m_e m_m G}{r}\left(\frac{1}{r} + \frac{2\sqrt{cH_{f2}}}{\sqrt{(m_e + m_m)G}}\right) . \tag{89}$$

It's necessary that F_{em}—as calculated in either reference frame—be equivalent. Referring back to Fig. 5, which shows a three-body system with no clear subsystem, the force between masses m_1 and m_2—as calculated via Eq. (70)—is consistent in both the two-body and three-body frames:

$$\begin{aligned}
H_{12} &= \frac{m_1 + m_2}{m_1 + m_2 + m_3} H_f \ , \\
F_{12a} &= \frac{m_1 m_2 G}{r}\left(\frac{1}{r} + \frac{2\sqrt{cH_{12}}}{\sqrt{(m_1 + m_2)G}}\right) , \\
F_{12b} &= \frac{m_1 m_2 G}{r}\left(\frac{1}{r} + \frac{2\sqrt{cH_f}}{\sqrt{(m_1 + m_2 + m_3)G}}\right) , \\
F_{12a} &= F_{12b} \ .
\end{aligned}$$

Recall that this is derived mathematically by enforcing consistency in the measurement of expansion rates with respect to arbitrary origins of expansion along a given vector. There doesn't seem to be any reason why this consistency should not be applicable in the case where two bodies of Fig. 5 happen to comprise a subsystem. Said another way, as shown by the above equations, the force between two bodies—as calculated in either the two- or three-body frames—is a function of all three masses and doesn't care how these bodies are moving relative to each other or whether they're part of a subsystem or not. Imagine a three-body system with chaotic motions where two bodies split off to form a subsystem. The forces between these bodies should be consistent immediately before and after the formation of this subsystem.

With this understanding, Eq. (88)—the relation for F_{em} in the three-body reference frame—and Eq. (89)—the relation for F_{em} in the two-body subsystem—can be considered equivalent. This, in turn, allows the following relation between the expansion parameter H_{f1} of the three-body frame and the parameter H_{f2} of the two-body frame to be written:

$$\begin{aligned}
\frac{H_{f2}}{m_e + m_m} &= \frac{H_{f1}}{m_s + m_e + m_m} \ , \\
H_{f2} &= \frac{m_e + m_m}{m_s + m_e + m_m} H_{f1} \ .
\end{aligned} \tag{90}$$

As expected, Eq. (90) parallels Eq. (81)—the equation above for H_{12}. Further, both Eqs. (81) and (90) are congruent with Eq. (69), restated below, when the reference mass m_r in this equation comprises two of the three bodies.

$$H_r = \frac{m_r}{m_t} H_f \ .$$

The observation that m_r in Eq. (69) can refer to a subsystem may not seem that interesting, but this actually has an important ramification—external mass can affect the gravitational forces within subsystems! Looking at Eq. (88), the presence of the Sun's mass m_s affects the force *between* the Earth and the Moon. It doesn't affect the Newtonian component of acceleration, which is purely a function of the Earth's and Moon's masses. It does, however, affect the expansion component, which is muted by the presence of the Sun. In actuality, it's muted by the total mass of the Solar System, which comprises the Sun, the planets, and the asteroid belt!

But the Solar System is a subsystem of the Milky Way, and therefore, the mass of the Milky Way must affect the forces within the Solar System—drastically reducing the expansion component relative to the Newtonian component. Traversing further up the hierarchy, the Milky Way is a member of the Local Group, which is, in turn, a member of the Virgo Supercluster, which is part of the Laniakea Supercluster complex.

To what extent does external mass affect internal systems? The universe has a lot of mass. Does all of this mass count? As the total system mass m_t in Eq. (70) goes to infinity, the expansion component asymptotically goes to zero. If m_t were set to the net mass of the universe, this effectively would be the case—the expansion-acceleration components in galaxies and clusters of galaxies would be reduced to insignificance.

However, we know that galaxies have flat rotation curves, and there are clusters where galaxies are mov-

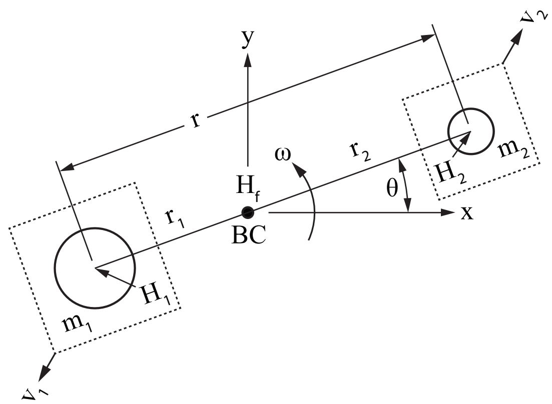

FIG. 8.

ing too quickly to be bound by Newtonian gravity. If non-Newtonian motion is to be explained by modified gravity—specifically, as it's described by Eq. (70)—it's not possible that the expansion parameters of galaxies and clusters are diluted by the entire mass of the universe.

X. EXPANSION PARAMETERS OF MOVING FRAMES

In the above relations, expansion parameters only ever equate to other expansion parameters—via distance or mass. There is no relation that describes expansion in a frame purely as a function of other metrics. So far, the mechanism by which expansion in a frame is manifested is unknown. Understanding this mechanism and how H_f relates to H_0 will be necessary to delve deeper into the mystery of flat galactic rotation curves and the motions of galaxies with respect to each other.

Fig. 8 shows the same two-body system from Fig. 4 with each body having a coincident frame that moves relative to the parent frame—the latter fixed at the barycenter BC of the system. The x and y coordinates of frame two—which is coincident with the barycenter of m_2—relative to the BC frame are thus:

$$x = r_2 \cos\theta \ ,$$
$$y = r_2 \sin\theta \ .$$

Taking the derivative of x and y with respect to time gives the following:

$$\dot{x} = \dot{r_2} \cos\theta - r_2\omega \sin\theta \ ,$$
$$\dot{y} = \dot{r_2} \sin\theta + r_2\omega \cos\theta \ ,$$

where

$$\omega = \dot{\theta} \ .$$

Taking the sum of the squares of $\dot{x}$ and $\dot{y}$ gives the square of the speed of frame two relative to BC:

$$ {v_2}^2 = \dot{x}^2 + \dot{y}^2 \ , \tag{91}$$
$$ {v_2}^2 = \dot{r_2}^2 + (r_2\omega)^2 \ . \tag{92}$$

Notice here, in Eq. (92), that speed v_2 squared is simply the sum of the squares of the radial and transverse components of vector $\vec{v}_2$.

Recall Eq. (55), which gives a relation between distance and mass for this two-body system. Taking the derivative of this equation with respect to time is thus:

$$r_2 = \frac{m_1}{m_2} r_1 \ ,$$
$$\dot{r_2} = \frac{m_1}{m_2} \dot{r_1} \ .$$

Plugging these equations into Eq. (92) gives this:

$$v_2 = \frac{m_1}{m_2}\sqrt{\dot{r_1}^2 + (r_1\omega)^2} \ .$$

With r_1 substituted for r_2, the speed of frame one—which is coincident with the barycenter of m_1—relative to the BC frame is similar to v_2:

$$v_1 = \sqrt{\dot{r_1}^2 + (r_1\omega)^2} \ .$$

Taking the ratio of the above two speed equations gives a result that intuitively parallels Eq. (55):

$$\frac{v_2}{v_1} = \frac{m_1}{m_2} \cancel{\frac{\sqrt{\dot{r_1}^2 + (r_1\omega)^2}}{\sqrt{\dot{r_1}^2 + (r_1\omega)^2}}} \ , \tag{93}$$
$$\frac{v_1}{v_2} = \frac{m_2}{m_1} \ . \tag{94}$$

Akin to Eq. (55), Eq. (93)—wherein the radial and transverse components of $\vec{v}_1$ and $\vec{v}_2$ cancel—shows that the ratio of v_2 to v_1 is irrespective of the paths of motion. Eq. (93) distills to Eq. (94), which shows that the relative speed between bodies one and two (and thus frames one and two) is purely a function of their masses.

Again, Eq. (94) is a natural extension of Eq. (55). If the distances relative to the barycenter of a system are a function of mass, then it follows that the derivatives of those distances—specifically, the derivatives of the distance vectors—with respect to time should obey the same relation. With this in mind, in general, if expansion parameters can be related via distance, they should also be relatable via speed.

Eq. (69) can be used to derive the ratio between the expansion parameters at m_1 and m_2:

$$H_1 = \frac{m_1}{m_t} H_f \ , \tag{95}$$

$$H_2 = \frac{m_2}{m_t} H_f \ , \tag{96}$$

$$\frac{H_1}{H_2} = \frac{m_1}{m_2} \ , \tag{97}$$

$$H_1 = \frac{m_1}{m_2} H_2 \ . \tag{98}$$

Similar to Eq. (69), Eqs. (97) and (98) can be regarded as general relations that relate the expansion parameter H_1 at the barycenter of m_1—representing a mass or collection of masses—to the expansion parameter H_2 at the barycenter of m_2—representing a second mass or collection of masses.

Plugging Eq. (94) into Eq. (98), relates expansion parameters to relative speeds:

$$\frac{H_1}{H_2} = \frac{v_2}{v_1} \ , \tag{99}$$

$$H_1 = \frac{v_2}{v_1} H_2 \ . \tag{100}$$

The interpretation of Eq. (100) is thus: An observer in reference frame two, moving with respect to the parent frame at BC, would measure a different expansion parameter relative to m_1 than would an observer in reference frame one relative to m_2—when their speeds differ—with the ratio of measured expansion parameters being equivalent to the ratio of their relative speeds.

Recognizing that speeds v_1 and v_2 are relative to BC—which is to say, relative to the parent frame—Eq. (99) can be extended as follows:

$$\frac{H_1}{H_2} \frac{r_f}{r_f} = \frac{v_2}{v_1} \ , \tag{101}$$

$$H_1 = \frac{v_2}{r_f} \ , \tag{102}$$

$$H_2 = \frac{v_1}{r_f} \ . \tag{103}$$

In these equations, for H_1 and H_2 to remain invariant for the two-mass system, r_f—which is termed the "frame size"—must vary in proportion to speeds v_1 and v_2. Further, this must happen instantaneously, which is to say, v_2 and r_f must vary proportionally in unison. Thus, it's imagined that r_f is a *combined* property that derives from the expansion parameter of a parent frame and the speed of a child frame moving relative to the parent.

Comparing Eq. (102) to Eqs. (61) and (63)—and Eq. (103) to Eqs. (60) and (62), gives this:

$$v_2 = r_f H_1 = r_2 H_f \ ,$$
$$v_1 = r_f H_2 = r_1 H_f \ .$$

Note that r in Eqs. (62) and (63) has been replaced by r_f in the above equations. In the top equation, v_2 corresponds to the same speed in two different contexts: In the context of Eq. (63), v_2 is the expansion rate of space as observed at m_2 in Fig. 4. In contrast, v_2, in Eq. (102), is the speed of m_2 relative to the parent frame. In both contexts, m_2 sees the same expansion parameter—H_1.

Hence, with this alternative perspective, the following relations are proposed:

$$H_f = \frac{v_x}{r_p} \ , \tag{104}$$

$$r_f = \frac{v_x}{H_p} \ , \tag{105}$$

$$r_p H_f = r_f H_p \ , \tag{106}$$

Subscript f, in these equations, refers to a child frame and p to the parent frame. Eq. (104) can be interpreted as thus: A child frame moving relative to a parent frame of frame size r_p at speed v_x has an expansion parameter of H_f. Here, r_p is defined as the distance where the expansion rate of space in a given frame is equivalent to the speed of a second frame moving with respect to the given frame. Conversely, Eq. (105) can be understood as: A child frame, moving at speed v_x relative to a parent frame with an expansion parameter of H_p, has a frame size of r_f. Eq. (106), which follows from Eqs. (104) and (105), parallels Eqs. (62) and (63).

The mention of a frame moving relative to a parent frame raises the question of relativistic effects. Relative to the moving frame, distances in the parent frame in the direction of motion will be length contracted, and relative to the parent frame, a clock in the moving frame will tick at a slower rate. At relativistic speeds—where v_x approaches c—do Eqs. (104) and (105) still hold?

In the parent frame, space—expanding from a point of origin a to a second point b across a proper distance of r_p—has an expansion rate of v_x at point b. The frame has an expansion parameter of H_f, and at v_x, proper distance r_p is traversed in time span t_f, which is proper time in the frame. This can be described by the following equation:

$$v_x = \frac{r_p}{t_f} = r_p H_f \ , \tag{107}$$

$$H_f = \frac{1}{t_f} \ . \tag{108}$$

Notice that Eq. (107) requires expansion parameter H_f to be defined as $1/t_f$.

In a child frame moving inertially relative to the parent frame—in parallel with r_p—the distance between points a and b—as measured as $r_p{}'$ in the child frame—is length contracted. With proper time in this frame defined as $t_f{}'$, the expansion parameter of the frame ${H_f}'$ is as follows:

$$ {r_p}' = \frac{1}{\gamma} r_p \ , \tag{109} $$

$$ t_f = \gamma {t_f}' \ , \tag{110} $$

$$ v_x = \frac{{r_p}'}{{t_f}'} = {r_p}' {H_f}' \ , \tag{111} $$

$$ {H_f}' = \frac{1}{{t_f}'} \ , \tag{112} $$

$$ {H_f}' = \gamma H_f \ , \tag{113} $$

$$ {r_p}' {H_f}' = \frac{1}{\gamma} r_p \gamma H_f = r_p H_f \ . \tag{114} $$

In Eq. (109), r_p is length contracted by Lorentz factor γ; and as given by Eq. (110), time ${t_f}'$, as measured by a clock in the child frame, is dilated by γ in the parent frame. With the expansion parameter defined as the inverse of time, ${H_f}'$—as given by Eq. (113)—is dilated relative to the parent frame's expansion parameter of H_f.

An observer in the child frame—looking at points a and b, while timing events with his own clock—would agree with an observer in the parent frame. Both would see space expanding at v_x at point b. Both would also agree on the expansion parameters in their respective frames—not on the absolute values, but on their values *relative* to their local clocks. As shown by Eqs. (108) and (112), each observer would see his expansion parameter as the inverse of the proper time in the frame. Thus, operatively—in terms of determining the rates of expansion—the expansion parameters in the parent and child frames are deemed to be equivalent.

Notice, for this to work, however—for contracted length ${r_p}'$ to be invariant with respect to direction—r_p must always be aligned with v_x, which is to say, in line with the direction of travel. This, however, is congruent with Eqs. (60) and (61)—where the expansion rate of space is in line with the distance across which it is expanding.

Thus, with the equivalence demonstrated by Eq. (114), either side of Eq. (106) can refer to parameters in the parent frame or the child frame. Taking this further, if Eqs. (104)–(106) are evaluated using parameters measured in the parent frame—where the parent frame is the rest frame—the physical effects of expanding space in the child frame are accurately described by those parameters, which is to say, these equations demonstrate Lorentz invariance.

Hence, looking at Eq. (104), for a given r_p, as v_x goes to zero, H_f goes to zero; and as v_x goes to c, it's reasoned that H_f must go to its maximum. Likewise, with Eq. (105)—for a given H_p—as v_x goes to zero, r_f goes to zero; and as v_x goes to c, r_f should go to its maximum. Again, all parameters, in these cases, may be measured in the parent frame. This will be further illustrated in the next section.

XI. THE EXPANSION PARAMETER—AS SEEN BY LIGHT

The standard interpretation of redshift is as follows: As a photon travels through space, over time, the expansion of space stretches the photon—increasing its wavelength. Increasing distance (and time) correlates with increasing redshift as described here:

$$ v = \dot{r} = r H_0 \ , \tag{115} $$

$$ \dot{\lambda} = \lambda H_0 \ . \tag{116} $$

Eq. (115) is Hubble's law, and Eq. (116) is Hubble's law applied to light, where λ is the emitted wavelength.

The expansion of space in the observable universe is given by the following equation:

$$ c = r_0 H_0 \ . \tag{117} $$

In Eq. (117), r_0 is typically termed the "Hubble radius", and it defines the radius of a sphere expanding at c—termed the "Hubble sphere". By definition, r_0 defines the information horizon—beyond which information is forever lost. In this way, it represents the maximum distance where information in our universe is preserved. Thus, concisely, r_0 defines the size of the "observable universe".

Given the arguments of the previous section, an alternative interpretation of redshift is thus: A child frame—moving with respect to an expanding parent frame—has an expansion parameter that relates to its speed and the frame size of the parent. As the speed of the child frame relative to the parent goes to c, the expansion parameter H_f goes to its maximum, and the frame size r_f goes to its maximum. Looking at Eq. (117), those maxima are H_0 and r_0—the expansion parameter and frame size of the parent frame, respectively.

Thus, it's posited that as the speed of the child frame v_x goes to c, its expansion parameter and frame size approach those values of the parent frame:

$$ \begin{aligned} & v_x \to c \ , \\ & H_f = \frac{v_x}{r_p} \to \frac{c}{r_0} \ , \\ & r_f = \frac{v_x}{H_p} \to \frac{c}{H_0} \ , \\ & H_f \to H_0 \ , \\ & r_f \to r_0 \ . \end{aligned} $$

In both interpretations, measuring the redshift of light informs the expansion rate of space, but they differ in terms of the underlying mechanism. A notable difference is that the present interpretation ascribes significance to the Hubble radius r_0—as r_0 is necessary to define the parent frame.

Looking at the Lorentz corrections from the previous section, as the child frame approaches c, a clock in that frame—relative to a clock in the parent frame—will slow to a tick rate approaching zero. Also, relative to the expansion parameter H_f—as measured in the parent frame—the expansion parameter $H_f{}'$ in the child frame will approach infinity. The physical effect on a photon is the same in either frame. In the parent frame, as $H_f \to H_0$, the photon is stretched over a time span of t. In the child frame, as $H_f{}' \to \infty$, the photon is stretched over a time span of $t' \to 0$. In both contexts, the resulting redshift—the physical effect of expansion—is the same.

1. *Hubble time*

Looking at Eqs. (108) and (112), the expansion parameter in a given frame is the inverse of proper time in the frame. If an expansion parameter approaches zero—it conceivably can—this would require that proper time in the frame approaches infinity. This is not to imply that this would be a physical time span. It's imagined that t_f in Eq. (108) is a virtual time span implicitly defined by its inverse, H_f. However, it's further imagined that Eq. (108) does describe how H_f evolves over time. As t_f increases, H_f decreases. Moreover, this would be the case for *every* reference frame in the universe.

Taking the inverse of H_0 gives the "Hubble time" t_0. The Hubble time has a definitive starting point—ostensibly the birth of the universe, which is to say t_0 is not a virtual time span. How closely does t_0 correspond to the age of the universe?

The estimated age of the universe is 13.787 billion years [3], which, working backwards, translates to a Hubble parameter equal to:

$$
\begin{aligned}
&t = 13.787 \times 10^9\,\mathrm{yr} \Rightarrow 435.075 \times 10^{15}\,\mathrm{s}\ , \\
&H_0 = 2.298 \times 10^{-18}\,\mathrm{m\,s^{-1}m^{-1}}\ , \\
&H_0 = 70.92\,\mathrm{km\,s^{-1}Mpc^{-1}}\ .
\end{aligned}
$$

Recent measurements of the Hubble parameter vary based on the chosen method, but they tend to fall within this range: 67-74 km s^{-1} Mpc^{-1} [19] [20], which averages to 70.5 km s^{-1} Mpc^{-1}. The agreement between this average and the calculated value above of 70.92 km s^{-1} Mpc^{-1} means that the Hubble time t_0 closely aligns with the estimated age of the universe.

The definition of H_0—as a function of Hubble time t_0—and its derivative with respect to t_0 is as follows:

$$H_0 = \frac{1}{t_0}\ , \tag{118}$$

$$\frac{dH_0}{dt_0} = \frac{-1}{{t_0}^2}\cancelto{1}{\frac{dt_0}{dt_0}}\ , \tag{119}$$

$$\dot{H}_0 = -{H_0}^2\ . \tag{120}$$

Thus the Hubble parameter H_0, as a function of Hubble time t_0, mathematically decreases according to Eq. (120).

XII. THE HUBBLE FRAME

All observers in their respective rest frames should see the information horizon—demarked by the Hubble radius r_0—receding at c. If the most distant coordinate recedes linearly at c, it follows that intermediate coordinates should also be receding at constant speed:

$$v = rH_0\ ,$$

$$\frac{dv}{dt} = \frac{dr}{dt}H_0 + r\frac{dH_0}{dt}\ , \tag{121}$$

$$\dot{v} = r{H_0}^2 - r{H_0}^2\ , \tag{122}$$

$$\dot{v} = 0\ . \tag{123}$$

At a given distance r between any two points in space, that distance expands according to Eq. (115), which is Hubble's law. Taking the derivative of Eq. (115) with respect to time gives Eq. (121). Plugging in Eq. (120) gives Eq. (122), which shows that the rate of speed increase at a given H_0 is canceled by the rate of H_0 decrease at a given distance—leaving the recessional speed constant over time. It stands to reason that if r_0 recedes at the constant rate of c, intermediate coordinates should recede at constant rates as well.

Bodies that move in sync with these receding coordinates—also referred to as "comoving" coordinates—are said to be moving in the "Hubble flow". This system of receding coordinates can be imagined as the cosmic rest frame or the "Hubble frame" for short. A body at rest in the Hubble frame would be seen as receding from an observer—also at rest in the frame—such that there was no relative speed or "peculiar speed" between the body and the coordinate coincident with that body—which is receding. Typically, however, bodies such as galaxies are found having peculiar speeds relative to the Hubble frame.

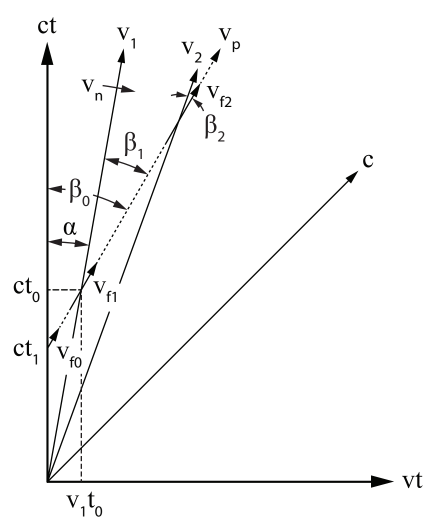

FIG. 9.

This system of moving coordinates can be visualized in Fig. 9, which is a spacetime diagram with time axis ct and space axis vt—where the rest frame is a coordinate in the Hubble frame. The rest frame, by definition, is only moving in time—along ct—while v_1, v_2, and c describe coordinates moving at varying speeds relative to the rest frame according to Eq. (115). These are termed "Hubble coordinates". It can also be imagined that v_1, v_2, and c represent the world lines of moving frames coincident with these coordinates. The inverse slope of a world line in the diagram ($vt/ct = v/c$) gives its speed relative to the rest frame. Thus, a line where $v = c$ is drawn at 45°.

Note that Fig. 9 only shows the right side of the complete spacetime diagram, which is mirrored about the ct axis. Imagine coordinates v_1, v_2, and c as all having mirrored counterparts—with the left and right c world lines establishing a light cone.

As demonstrated by Eq. (123), the recessional speed of any given Hubble coordinate remains constant over time; and thus, in the diagram, the world lines for these coordinates are drawn with straight lines. Notice that, when the clocks of these world lines are all run in reverse, the world lines all converge at a point in spacetime that signifies the universe's initial event. Accordingly, an observer in the rest frame of any Hubble coordinate, moving backwards in time along the ct axis, would see bodies in the Hubble flow converging on his location, making it appear to the observer that he is at the center of the observable universe.

The world line of an inertial frame moving at speed v_p relative to the rest frame of a Hubble coordinate is also drawn in the diagram. Notice that the v_p world line does not intersect the point of convergence of Hubble coordinates. However, an observer in the v_p rest frame would also see the observable universe as expanding at c. This frame would have its own light cone—with coordinates converging at a point in the past, marking the initial event in the frame.

Yet, it's reasoned that the universe could have had only **one** initial event. As such, it's proffered that this event and its light cone establish the Hubble frame. Further, because every Hubble coordinate has its own light cone that emanates from this initial event, the Hubble frame can generally be imagined as the rest frame of *any* Hubble coordinate.

While there can be no concept of position in the Hubble frame—what would the position be relative to?—there is a concept of speed relative to this frame. For example, an observer moving at a peculiar speed of v_p in the diagram would see blueshift in light observed from the right side of the ct axis of the coincident Hubble coordinate and redshift from the opposite direction. We see this effect—based on our motion in the Milky Way and the Milky Way's peculiar speed—as a dipole in the CMB where one side of a spherical survey is slightly blueshifted relative to the other. Thus, an observer at rest in the Hubble frame should see no dipole.

Notice that the v_p world line crosses coordinates in the Hubble frame at angles that decrease over time starting with β_0—relative to the rest frame, followed by β_1 relative to v_1, and finally β_2 with respect to v_2. Decreasing angles translate to decreasing relative speeds, and thus, the frame moving along the v_p world line is decelerating with respect to coordinates in the Hubble frame—which is to say, decelerating in the Hubble frame.

As the frame moving at v_p intersects a Hubble coordinate, its speed relative to that coordinate is defined as v_f. Specifically, v_f is defined as the peculiar speed relative to the coincident Hubble coordinate. More broadly, v_f can be understood as the peculiar speed relative to the overall Hubble flow (or Hubble frame). This is in contrast to v_p, which is defined as the speed with respect to a fixed Hubble coordinate.

This can be visualized in the diagram. Notice that the v_p world line is broken into a series of segments: v_{f0}, v_{f1}, and v_{f2}—where each segment represents the peculiar speed v_f at the coincident Hubble coordinate. At time t_1—where the frame moving at v_p crosses the ct axis of the rest frame, v_{f0} is equivalent to v_p—as evidenced by both segments having the same angle β_0 with respect to the Hubble coordinate. At the point where the moving frame intersects coordinate v_1, relative to v_1, v_f has decelerated to v_{f1}; and at v_2, relative to v_2, v_f has further slowed to v_{f2}.

As the moving frame continues along the v_p world line, it will asymptotically approach the slope of the Hubble-frame coordinate of the same slope—which is to say the same speed. After an infinite amount of time, the moving frame will come to rest in the Hubble frame. Light, with a v_p of c, will asymptotically approach the edge of the light cone—defined by the c coordinate in the diagram. Keeping in mind that the diagram is mirrored, there is no direction where a frame with a non-zero peculiar speed will not decelerate relative to the Hubble frame.

As the v_p world line crosses the v_1 coordinate, v_1 becomes the rest frame, which would look identical to the frame of Fig. 9—always with r_0 receding at c. Relative to this frame, the peculiar speed would not be v_{f0} but v_{f1}—and the blueshift in the dipole would be slightly less than before.

From the diagram, the following equation can be written:

$$v_n t_0 = v_p(t_0 - t_1) \ . \tag{124}$$

As time progresses, coordinate v_n rotates clockwise about the origin—tracking the v_p world line as it intersects Hubble coordinates. At time t_0, v_n has rotated an angle α relative to time axis ct and is coincident with v_1—which is to say, at t_0, v_n is equivalent to v_1. Looking at the diagram, in the time span $t_0 - t_1$, a particle moving at speed v_p will have traveled the same distance as a particle moving at the current value of v_n—which is v_1. With t_0 defined as the Hubble time, v_n and t_0 in Eq. (124) are dynamic with respect to time, while v_p and t_1 are constant.

Taking the derivative of Eq. (124) with respect to time gives the following:

$$\frac{dv_n}{dt}t_0 + v_n \cancelto{1}{\frac{dt_0}{dt}} = \cancelto{0}{\frac{dv_p}{dt}}(t_0 - t_1) + v_p\left(\cancelto{1}{\frac{dt_0}{dt}} - \cancelto{0}{\frac{dt_1}{dt}}\right) , \tag{125}$$

$$\dot{v}_n t_0 + v_n = v_p . \tag{126}$$

In the above equations, dt and dt_0 are asserted to be equivalent. As noted, the Hubble time and estimated age of the universe are equivalent within the margin of error, and it's imagined that rates of change of these times—at least in the current epoch—are essentially equivalent. Further, in the context of the observable universe, these rates may have *always* been exactly equivalent, but that is a different discussion.

Speed v_p is constant in the rest frame over time, and thus, dv_p/dt goes to zero. With these considerations, Eq. (125) reduces to Eq. (126).

Plugging Eq. (118)—the relation between Hubble time t_0 and the Hubble parameter H_0—into Eq. (126), gives this:

$$\dot{v}_n \frac{1}{H_0} + v_n = v_p , \tag{127}$$

$$\dot{v}_n = (v_p - v_n)H_0 . \tag{128}$$

In the diagram, at time t_1, the coincident coordinate v_n is in line with the ct axis of the rest frame and thus has a speed of zero in the frame. With this in mind, the following equations are written:

$$v_f = v_p - \cancelto{0}{v_n} , \tag{129}$$

$$\dot{v}_n = (v_f - \cancelto{0}{v_n})H_0 = v_f H_0 , \tag{130}$$

$$v_f \cancel{H_0} = (v_p - v_n)\cancel{H_0} , \tag{131}$$

$$v_f = v_p - v_n , \tag{132}$$

$$\dot{v}_f = \cancelto{0}{\dot{v}_p} - \dot{v}_n , \tag{133}$$

$$a_f = \dot{v}_f = -v_f H_0 . \tag{134}$$

In Eq. (129), at a v_n of zero, v_f is equivalent to v_p. This is shown in the diagram where v_{f0} and v_p have the same slope relative to the ct axis—and thus the same speed. With Eq. (129), Eq. (128) can be rewritten as Eq. (130), which gives the acceleration of the floating coordinate v_n as it traces the moving frame in the reference frame of the coincident Hubble coordinate—which is to say the Hubble frame.

Plugging Eq. (130) into Eq. (128) gives Eq. (131), which reduces to Eq. (132). Notice the inclusion of the v_n term in Eq. (132), which correctly indicates that after an infinitesimal amount of time, v_f will be slightly smaller than v_p. Importantly, because v_f is always relative to the reference frame of the coincident coordinate, which changes over time, this equation is only valid within this infinitesimal time period. Taking the derivative of Eq. (132) with respect to time gives Eq. (133), where, as before, $\dot{v}_p$ is zero. Akin to Eq. (132), Eq. (133) is only correct for an infinitesimal span of time.

Eq. (134), which follows from Eqs. (130) and (133), gives the deceleration a_f of a frame moving relative to the coincident Hubble coordinate—which is to say deceleration in the Hubble frame—as a function of its peculiar speed v_f in the frame. Because both v_f and a_f are always measured in the frame of the coincident coordinate, Eq. (134) is deemed to be generally valid. Notice that both v_f and a_f are scalars. In the specific case where the peculiar speed of a given frame is zero, that frame is considered to be at rest in the Hubble frame.

Notice further that in static—non-expanding—space, which is described by an H_0 of zero in Eq. (134), there is no deceleration. A static universe—where H_0 goes to zero—would be of infinite age and size—and *frameless*. In contrast, the present model holds that the observable universe—the volume within which information is preserved—is finite and perpetually expanding at c. It's surmised that this constitutes a frame against which peculiar speed v_f and acceleration a_f can be defined.

XIII. MASS OF THE OBSERVABLE UNIVERSE

Eq. (134), when applied to light, holds that a photon is decelerated in the Hubble frame as follows:

$$a_f = -cH_0 . \tag{135}$$

This deceleration, which can be described as a photon losing energy over time as it travels through expanding space, manifests as redshift.

The following equations explore the idea that the redshift of a photon can be equivalently imagined in two different contexts: traveling through expanding space and traveling against a decelerating field:

$$\dot{\lambda} = \lambda H_0 ,$$

$$p = \frac{h}{\lambda} , \tag{136}$$

$$\dot{p} = \frac{-h}{\lambda^2}\dot{\lambda} , \tag{137}$$

$$\dot{p} = \frac{-h}{\lambda^{\cancel{2}}}\cancel{\lambda}H_0 , \tag{138}$$

$$m_e a_f = \dot{p} = \frac{-h}{\lambda}H_0 , \tag{139}$$

$$m_e = \frac{E}{c^2} = \frac{p}{c} = \frac{h}{c\lambda} , \tag{140}$$

$$\frac{\cancel{h}}{\cancel{\lambda}}\frac{1}{c}a_f = -\frac{\cancel{h}}{\cancel{\lambda}}H_0 , \tag{141}$$

$$a_f = -cH_0 .$$

Eq. (116), which gives Hubble's law applied to the wavelength of light, is restated above. The momentum of a photon as a function of wavelength is given by Eq. (136) and the change in momentum over time $\dot{p}$ by Eq. (137).

Plugging Eq. (116) into Eq. (137) gives Eq. (138), which reduces to Eq. (139)—the latter relating the effective mass of a photon m_e and deceleration a_f to the change in momentum. With the definition of m_e in Eq. (140), Eq. (139) distills to Eq. (135).

Referring back to Eq. (21), acceleration implies time uncertainty. Equating this relation with the deceleration of a photon in the Hubble frame—as given by Eq. (135)—yields the following:

$$\cancel{c}H_0 = \frac{2\cancel{c}}{\Delta t_u} \ , \tag{142}$$

$$H_0 = \frac{1}{t_0} = \frac{2}{\Delta t_u} \ , \tag{143}$$

$$\Delta t_u = 2t_0 \ . \tag{144}$$

To clarify the applicability of Eq. (21) in this case—space itself is modeled as a field with time uncertainty Δt_u at all points therein. A photon moving at c relative to space—which is to say the Hubble frame—sees acceleration opposite the direction of travel. The photon here is the carrier of information (vs. the field in previous cases), and in keeping with the general principle of Eq. (21), acceleration is opposite the direction of information flow. As both accelerations in Eq. (142) are relative to the Hubble frame (and are both redshifting accelerations), they may be directly equated.

Plugging Eq. (119) into Eq. (142) gives Eq. (144). Eq. (144) asserts that the time uncertainty of the observable universe Δt_u is double the Hubble time t_0. Notably, this time uncertainty will *always* be double the age of the observable universe. Is the time and energy of the universe perpetually on loan—one that never expires? Is the universe a vacuum fluctuation? In 1973, this question was originally posed by Edward Tryon in a paper of the same title [21].

With the relation between H_0 and time uncertainty Δt_u given by Eq. (143), the energy uncertainty of the observable universe E_u is derived via the uncertainty principle:

$$\Delta E_u \Delta t_u \geq \frac{\hbar}{2} \ ,$$

$$\Delta t_u = \frac{2}{H_0} \ ,$$

$$\Delta E_u \frac{2}{H_0} \geq \frac{\hbar}{2} \ , \tag{145}$$

$$\Delta E_u = \frac{\hbar H_0}{4} \ . \tag{146}$$

As before, replacing the $\geq$ sign with an equals sign in Eq. (146) pins ΔE_u at its minimum.

To recap, each observer in his respective rest frame will see the sphere that contains all of the information in that frame expanding at c. All points within this sphere have time and energy uncertainties as described by Eqs. (144) and (146), respectively. As such, Eq. (7) may be used to calculate the mass within that sphere—which is to say the mass of the observable universe:

$$\Delta E_u = \frac{m_0 h G}{8\pi {r_0}^2 c} \ , \tag{147}$$

$$\Delta E_u = \frac{m_0 \hbar G}{4{r_0}^2 c} \ , \tag{148}$$

$$\frac{m_0 \cancel{\hbar} G}{\cancel{4}{r_0}^2 c} = \frac{\cancel{\hbar} H_0}{\cancel{4}} \ , \tag{149}$$

$$m_0 = \frac{c H_0 {r_0}^2}{G} \ , \tag{150}$$

$$r_0 = ct_0 = \frac{c}{H_0} \ , \tag{151}$$

$$m_0 = \frac{c\cancel{H_0}c^2}{GH_0^{\cancel{2}}} \ , \tag{152}$$

$$m_0 = \frac{c^3}{GH_0} = \frac{c^3 t_0}{G} \ . \tag{153}$$

Eq. (7) is restated as Eq. (147) with m_0 and r_0 corresponding to the mass and radius of the observable universe in a given frame. In Eq. (149), Eq. (148) is equated with Eq. (146), which, via Eq. (117), reduces to Eq. (153). Eq. (153) shows that the mass of the observable universe m_0 is directly proportional to the Hubble time t_0 and thus inversely proportional to the Hubble parameter H_0.

With an H_0 of 70 km s^{-1} Mpc^{-1}, m_0 calculates to:

$$H_0 = 70\,\mathrm{km\,s^{-1}Mpc^{-1}} \ ,$$
$$H_0 = 2.27 \times 10^{-18}\,\mathrm{m\,s^{-1}m^{-1}} \ ,$$
$$m_0 = 1.78 \times 10^{53}\,\mathrm{kg} \ .$$

Note that Eq. (153) has previously been arrived at via other lines of reasoning [22][23]. For example, the relation between mass density ρ_0 and H_0—which emerges from the Friedmann model of an expanding universe [24]—reduces as follows:

$$G\rho_0 \simeq {H_0}^2 \ ,$$
$$m_0 \sim \rho_0 {r_0}^3 \ ,$$
$$r_0 = \frac{c}{H_0} \ ,$$
$$m_0 \sim \frac{\cancel{H_0}^2}{G}\frac{c^3}{H_0^{\cancel{3}}} \ ,$$
$$m_0 \sim \frac{c^3}{GH_0} \ .$$

With Eq. (153) and mass–energy equivalence, the energy of the observable universe E_0 is thus:

$$E_0 = m_0 c^2 \ ,$$

$$E_0 = \frac{c^5 t_0}{G} = \frac{c^5}{GH_0} \ . \tag{154}$$

Taking the derivative of E_0 with respect to time gives this:

$$\frac{dE_0}{dt} = \frac{c^5}{G}\cancelto{1}{\frac{dt_0}{dt}} \quad , \tag{155}$$

$$P_0 = \frac{c^5}{G} \ . \tag{156}$$

Eq. (156), which gives the rate at which energy is added to the observable universe, is recognizable as the Planck power—theoretically, the upper power limit in the observable universe. Interestingly, there are no parameters in this equation—only constants.

XIV. EXPANSION PARAMETERS IN THE HUBBLE FRAME

In Section X, it was shown that a frame moving relative to a parent frame has an expansion parameter that is a function of the moving frame's speed in the parent frame and the parent frame's expansion parameter. In Section XI, this idea was extrapolated to the redshift of light—where a frame moving at c relative to the parent frame, which is to say the Hubble frame, sees the full expansion parameter of the parent frame, which, in the case of the Hubble frame, is H_0.

It's thus imagined that a frame moving less than c in the Hubble frame would see an expansion parameter less than H_0. This aligns with the findings of Section XII, which show that frames moving at peculiar speeds in the Hubble frame are decelerating in the frame in proportion of the peculiar speed. It's imagined that the physical effect of this deceleration is expansion in the moving frame—where a frame with a peculiar speed of zero is not decelerating and has an expansion parameter of zero.

Applying Eqs. (104) and (105) to a frame moving at subluminal speed v_x relative to the Hubble frame gives the following:

$$H_f = \frac{v_x}{r_0} \ , \tag{157}$$

$$r_f = \frac{v_x}{H_0} \ , \tag{158}$$

$$r_0 H_f = r_f H_0 \ , \tag{159}$$

$$v_f = r_f H_f \ , \tag{160}$$

$$v_f = \frac{{v_x}^2}{r_0 H_0} \ , \tag{161}$$

$$v_f = \frac{{v_x}^2}{c} \ , \tag{162}$$

$${r_f}' {H_f}' = r_f H_f \ . \tag{163}$$

Eq. (160) defines speed v_f as the speed of expansion in the child frame using the parameters of the child frame—frame size r_f and expansion parameter H_f. With the definition of frame size from Section X, v_f is also the speed of an observer moving relative to r_f—where that observer sees an expansion parameter of H_f. In Eq. (157) that speed (v_x) is measured in the parent frame. Whereas in Eq. (160), the speed in question (v_f) is measured in the child frame. As a quick sanity check—looking at Eq. (162), which relates speed v_f to v_x—as v_x goes to c, v_f goes to c.

However, to say that speed v_f is the speed of an observer relative to r_f is tantamount to measuring one's speed in one's own reference frame—which seems like a non sequitur. For example, speed v_x in Eq. (107) is measured with respect to distance r_p, which is a distance in the parent frame. Here, speed v_f is measured with respect to r_f, which is a distance is the rest frame of the observer. If the rest frame moves with the observer, how can distance r_f ever be traversed?

But this is exactly the scenario described in Section XII, where speed v_f is measured relative to the coincident Hubble coordinate—which is *always* coincident! Akin to v_f in the Hubble frame, with r_f as a parameter of the Hubble frame—in an infinitesimal amount of time, across an infinitesimal distance—a speed of v_f relative to r_f can be determined. Hence, speed v_f in Eq. (162) is reasoned to be the same quantity as peculiar speed v_f in Eq. (134).

Lastly, in congruence with Eq. (114), the product of ${r_f}'$ and ${H_f}'$—which are the Lorentz-corrected frame parameters as seen by an observer in the child frame moving in the parent frame—is equivalent to the product of those parameters as measured in the parent frame. Thus, as before, the physical effect of expansion in the child frame is Lorentz invariant.

Plugging Eqs. (162) and (117) into Eq. (157) gives a relation between peculiar speed v_f and H_f:

$${H_f}^2 = \frac{{v_x}^2}{{r_0}^2} \ ,$$

$${H_f}^2 = \frac{v_f c}{\cancel{{r_0}^2}} \frac{\cancel{{r_0}^2} {H_0}^2}{c^2} \ ,$$

$$H_f = \sqrt{\frac{v_f}{c}} H_0 \ . \tag{164}$$

Hence, as shown by Eq. (164), a frame moving at peculiar speed v_f in the Hubble frame sees an expansion parameter of H_f. As v_f goes to zero, H_f goes to zero. This aligns with Eq. (134), where deceleration a_f also goes to zero as peculiar speed v_f goes to zero. At the other end of the spectrum—as v_f goes to c, H_f goes to H_0.

With Eqs. (158) and (162), frame size r_f relates to v_f as follows:

$${r_f}^2 = \frac{{v_x}^2}{{H_0}^2} \ ,$$

$${r_f}^2 = \frac{v_f c}{{H_0}^2} \ ,$$

$$r_f = \frac{\sqrt{v_f c}}{H_0} \ . \tag{165}$$

As shown by Eq. (165), as v_f goes to zero r_f goes to zero, and as v_f goes to c, r_f goes to r_0—the extent of the observable universe.

Multiplying Eq. (158) by H_f relates v_f and v_x in terms of acceleration.

$$r_f H_f = \frac{v_x}{H_0} H_f \ ,$$
$$v_f H_0 = v_x H_f \ , \tag{166}$$

Looking at Eq. (134), Eq. (166 shows that a frame with a peculiar speed of v_f in the Hubble frame (with an expansion parameter of H_0) decelerates at the same rate as a frame with a peculiar speed of v_x in a frame with an expansion parameter of H_f.

XV. GALACTIC ROTATION CURVES

In this section, Eq. (70) is applied to a selection of nearby galaxies from the SPARC (Spitzer Photometry & Accurate Rotation Curves) database to derive their rotation curves—where H_f in this equation is tuned to provide the best curve fit. Each value for H_f is plotted against the galaxy's published peculiar speed v_f to see if the resulting data point comports with Eq. (164).

$$a_n = \frac{m_r G}{r} \left(\frac{1}{r} + \frac{2\sqrt{cH_f}}{\sqrt{m_t G}} \right) \ ,$$
$$H_f = \sqrt{\frac{v_f}{c}} H_0 \ .$$

The SPARC database comprises a large catalog of galaxies that vary in mass, gas fraction, effective radii, and surface brightness [25]. As a cohesive dataset spanning a broad range of morphologies, the SPARC data provide an ideal test of modified-gravity as well as dark-matter halo models—the latter being the primary focus of the cited paper.

A subset of the catalog was selected to be examined based on proximity to the Milky Way—where galaxies within a distance of roughly 5 Mpc were included. A complete description of this analysis and the rotation curve for each galaxy—as derived via Eq. (70)—is provided in a separate document [26]. The software used to model these galaxies is publicly available at the URL in the citation and is free to use under the MIT license.

In short, disks are modeled as zero-thickness plates of varying density with respect to radius. Bulges are modeled as spheres where density varies according to radius. Discs and bulges are broken into finite elements, and Eq. (70) is solved for each element, where r is the distance from the center of mass of that element to an offset from the center of rotation. The net acceleration a_n—toward the center of rotation—at a given offset is the vector sum of the accelerations with respect to each disk and bulge element. Net acceleration a_n is solved across a range of offsets for a given galaxy from the inner to the outermost data points—thereby establishing a rotation curve.

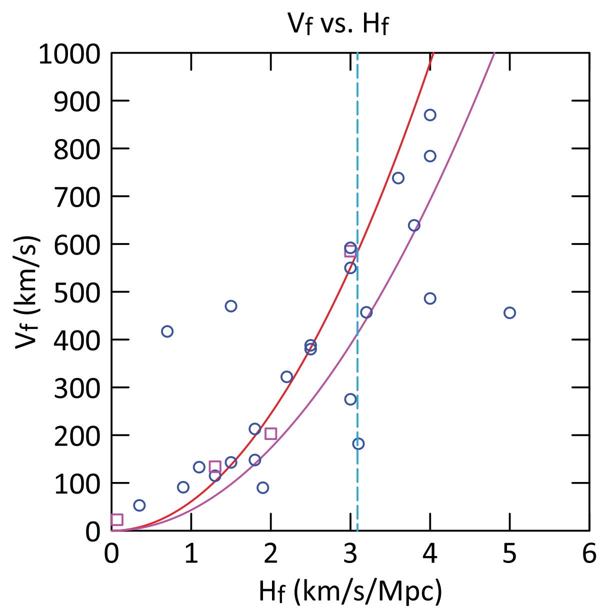

FIG. 10.

Looking at Eq. (70), when applied to galaxies, there are two free parameters: m_t, which is the total galactic mass, and H_f, which is the expansion parameter of the moving frame containing the galaxy. The total mass m_t is constrained by estimates of the matter comprising the stellar populations, dust, and gas. This is derived from the Newtonian curves in the SPARC data. H_f was adjusted individually for each galaxy to generate the rotation curve that best fit the error bars of the published data.

Fig. 10 is a plot of peculiar speed v_f vs. expansion parameter H_f for the 29 galaxies included in the analysis. Circles in the figure indicate fair to excellent curve fits, while squares denote poor curve fits—the latter having a count of four.

Peculiar speeds for these galaxies were sourced from the *NASA/IPAC Extragalactic Database* [27]. Ostensibly, if both the radial and transverse velocities of a distant galaxy were known, its true velocity relative to the Milky Way could be derived, which in turn would allow its true peculiar speed relative to the CMB to be determined. Given the challenge with determining transverse velocities [28], it's assumed the estimated peculiar speeds listed in the Extragalactic Database were solely based on radial components. The spread between the left and right curves in Fig. 10—which trace Eq. (164)—is meant to account for this uncertainty. Given a large enough data set, if Eq. (164) is valid, it seems reasonable that data points should concentrate along these curves. In the small set of analyzed galaxies, about 83% comport with the expected trend.

1. The Milky Way

As r goes to infinity in Eq. (70), the reference mass m_r approaches the total mass m_t—as the galaxy looks increasingly like a point mass to an orbiting particle. Thus, at large distances, Eq. (70) reduces to Eq. (37) as follows:

$$
\begin{aligned}
& a_n = \frac{m_r G}{r}\left(\frac{1}{r} + \frac{2\sqrt{cH_f}}{\sqrt{m_t G}}\right) \ , \\
& m_r \to m_t \ , \\
& a_n = \cancelto{0}{\frac{m_t G}{r^2}} + \frac{2\sqrt{cH_f m_t G}}{r} \ , \\
& a_n = \frac{2\sqrt{cH_f m_t G}}{r} \ , \\
& \frac{{v_{flat}}^2}{\cancel{r}} = \frac{2\sqrt{cH_f m_t G}}{\cancel{r}} \ , \\
& v_{flat} = \sqrt{2}(cH_f m_t G)^{\frac{1}{4}} \ . \qquad (167)
\end{aligned}
$$

Note that as m_t approaches a point mass, the local expansion parameter H_l—as seen by a particle of negligible mass in the field—approaches the frame's expansion parameter H_f. Further, in this regime, the Newtonian component of Eq. (37) loses significance in relation to the expansion component and thus, at a certain distance, this can be ignored. Here, Eq. (37) reduces to Eq. (36). Assuming circular motion, Eq. (167) gives the asymptotic speed v_{flat} that is approached by particles as the expansion component of centripetal acceleration becomes dominant.

Fitting the Milky Way's rotation curve is left as a future exercise, but with an estimate of its peculiar speed v_f and (baryonic) mass m_t [29], the following parameters are easily calculated: H_f, k_f, and v_{flat}.

$$
\begin{aligned}
& m_t = 8.43 \times 10^{10}\,\mathrm{M}_\odot = 1.68 \times 10^{41}\,\mathrm{kg} \ , \\
& v_f = 565\,\mathrm{km\,s^{-1}} \ , \\
& H_f = 3.04\,\mathrm{km\,s^{-1}Mpc^{-1}} \ , \\
& k_f = 5.88 \times 10^{-61}\,\mathrm{kg^{-1}s^{-1}} \ , \\
& v_{flat} = 191\,\mathrm{km\,s^{-1}} \ .
\end{aligned}
$$

The parameter v_{flat} predicts that the Milky Way's rotation curve flattens to roughly 191 km s^{-1}, which is consistent with recent observations that extend out to 25 kpc [30][31]. Yoshiaki Sofue has compiled a "grand" rotation curve for the Milky Way that extends out to 400 kpc [32]. From 40 to 100 kpc, v_{flat} aligns well with this curve. Beyond 100 kpc, uncertainty in the data increases, and the error bars encompass a wide range of rotational velocities—from roughly 100 to 200 km s^{-1}.

Here, a new constant, termed the "frame constant", is introduced that is defined as the expansion parameter per unit mass. It combines the ratio of H_f to m_t in Eq. (70) into one parameter that applies to all particles in a given system:

$$k_f = \frac{H_i}{m_i} = \frac{H_f}{m_t} \ . \qquad (168)$$

With Eq. (168), Eq. (70) can be simplified as follows:

$$
\begin{aligned}
& k_f = \frac{H_i}{m_i} = \frac{H_f}{m_t} \ , \\
& a_n = \frac{m_r G}{r}\left(\frac{1}{r} + 2\sqrt{\frac{c}{G}k_f}\right) \ , \qquad (169) \\
& a_n = \frac{m_r G}{r^2} + \frac{2}{r}\sqrt{\frac{c}{G}k_f} \ , \qquad (170) \\
& k_e = \frac{2}{\cancel{r}}\sqrt{\frac{c}{G}k_f}\left(\frac{r^{\cancel{2}}}{m_r G}\right) \ , \qquad (171) \\
& k_e = \frac{2r}{m_r G}\sqrt{\frac{c}{G}k_f} \ . \qquad (172)
\end{aligned}
$$

Plugging Eq. (168) into Eq. (70) gives Eq. (170), which defines a_n as the sum of the Newtonian and expansion components of acceleration. k_e, in Eq. (172), is the ratio of these components, which is an indication of their relative strength. Notice that k_e, which is a function of r, shows that the transition from the Newtonian to expansion-acceleration regime is linear with respect to distance.

When applied to the Solar System, Eq. (172) shows that the acceleration regime is entirely Newtonian:

$$
\begin{aligned}
& m_r = 1\,\mathrm{M}_\odot = 1.988\,47 \times 10^{30}\,\mathrm{kg} \ , \\
& r = 1\,\mathrm{AU} = 149\,597\,870.7\,\mathrm{km} \ , \\
& k_e = 3.66 \times 10^{-30} \ .
\end{aligned}
$$

At the average radius of Earth's orbit, the Newtonian component is 30 orders of magnitude larger than the expansion component.

At 4.25 ly—the distance to Proxima Centauri, the expansion component is still negligible at 25 orders of magnitude less than the Newtonian component:

$$
\begin{aligned}
& r = 4.2465\,\mathrm{ly} = 4.017 \times 10^{13}\,\mathrm{km} \ , \\
& k_e = 9.84 \times 10^{-25} \ .
\end{aligned}
$$

Clearly, the effects of modified gravity are not detectable in or near the Solar System, where motions, within the precision of our measurements, remain Newtonian—with the one caveat being the precession of Mercury, where a relativistic correction must be included in the calculation to reconcile the predicted and measured precession [33].

2. MOND

Well before Proxima Centauri—at around .111 ly (7300 AU), the strength of the Sun's gravitational field drops below the MOND constant a_0 of 1.2E−10 m s^{-2}. According to MOND, as discussed, this constant marks the transition to the non-Newtonian acceleration regime, but, as just demonstrated, the Sun's gravity remains Newtonian well past Proxima Centauri! In principle, MOND *does* account for such scenarios with a concept called the "external-field effect" (EFE)—where modified gravity is muted in systems that are in the presence of relatively strong external fields.

In contrast, under the present thesis, non-Newtonian effects in a galaxy are quantified by the frame constant k_f—which applies to all bodies and systems of bodies that are gravitationally bound to and part of the host galaxy. Looking at the Milky Way, at small scales—the scale of our Solar System and even out to nearby stars, k_f is too small for non-Newtonian effects to be observed. Non-Newtonian motion is only observed at galactic scales—where distances are such that the non-Newtonian acceleration component is dominant.

The vertical dashed cyan line in Fig. 10 is drawn at an H_f of 3.09 km s^{-1} Mpc^{-1}, which is the value of H_f that corresponds to the MOND constant a_0 of 1.2E−10 m s^{-2}. Equating the deep-MOND-regime relation, Eq. (38), with Eq. (36), distills as follows:

$$
\begin{aligned}
&\frac{\sqrt{a_0 \cancel{m_t} G}}{\cancel{r}} = \frac{2\sqrt{c H_M \cancel{m_t} G}}{\cancel{r}} \ , \\
&a_0 = 4 c H_M \ , \\
&H_M = \frac{1}{4c} a_0 \ , \\
&H_M = 3.09\,\mathrm{km\,s^{-1} Mpc^{-1}} \ .
\end{aligned}
$$

The expansion parameter corresponding to the MOND constant a_0 is designated as H_M. With Eq. (164), H_M equates to a frame speed v_M of 583 km s^{-1}, which is where the dashed blue line intersects the left red curve in Fig. 10. The blue line intersects the right magenta curve at 412 km s^{-1}. Interestingly, the Milky Way's peculiar speed of 565 km s^{-1} is near v_M, and correspondingly, its expansion parameter of 3.04 km s^{-1} Mpc^{-1} is close to H_M. The MOND constant a_0 was arrived at empirically and is the number that yields the best curve fits—on average—for the many galaxies tested against MOND. Ultimately, is a_0 a gauge of the average peculiar speed of galaxies in the cosmos?

XVI. THE LOCAL GROUP

The salient question in Section IX was: "To what extent does external mass affect internal systems"? In Section IX, it was shown that the expansion parameter of a system, which may have subsystems, gets evenly distributed to all of the mass in the system. But what defines a system?

Here, a system is defined as a hierarchy of bodies and materials in stable orbits—where, looking from the top down, any given body may comprise a subsystem of other bodies. Assuming the system remains isolated (and loses no energy over time), these bodies move in unison and will continue to do so indefinitely. As such, all of the particles in a system are deemed to be interconnected. Crucially, it is reasoned that **all particles comprising the *complete* system, which collectively move in a frame, share the same frame constant k_f.**

The immediate follow-on question is: In a hierarchy of systems, what constitutes the top node? Is this typically a galaxy? A cluster of galaxies? To dig into this question, the main galaxies in the Local Group—Andromeda, Triangulum, and the Milky Way—are investigated to see where the evidence points. Eq. (69) shows that as mass is added to a system, the expansion parameter of a reference mass in that system decreases in concert. In general, this relation can be used as a starting point to explore the effects of combining galaxies into a system.

For example, if the Milky Way and Andromeda comprised a system, the Milky Way's expansion parameter H_f, estimated above at 3.04 km s^{-1} Mpc^{-1}, would be diluted by the system mass m_t, which would now include Andromeda's mass:

$$
\begin{aligned}
H_r &= \frac{m_r}{m_t} H_f \ , \\
v_{flat} &= \sqrt{2 m_r} \left(\frac{c H_r G}{m_t} \right)^{\frac{1}{4}} \ . \qquad (173)
\end{aligned}
$$

Also, note that Eq. (167), the relation for v_{flat}, takes a different form when the reference mass is only a portion of the system mass:

Assuming that the Milky Way and Andromeda are of roughly equal mass [34], which is fair for a back-of-the-envelope calculation, m_r, which corresponds to the Milky Way here, and m_t are as follows:

$$
\begin{aligned}
m_r &= 1.68 \times 10^{41}\,\mathrm{kg} \ , \\
m_t &= 3.36 \times 10^{41}\,\mathrm{kg} \ .
\end{aligned}
$$

As a rough estimate, the peculiar speed v_f of the two-galaxy frame is assumed to be that of the Milky Way, which leaves the frame constant H_f for the system at 3.04 km s^{-1} Mpc^{-1}.

$$
\begin{aligned}
v_f &= 565\,\mathrm{km\,s^{-1}} \ , \\
H_f &= 3.04\,\mathrm{km\,s^{-1} Mpc^{-1}} \ .
\end{aligned}
$$

With these new parameters, the following metrics for the Milky Way recalculate as follows:

$$
\begin{aligned}
H_r &= 1.52\,\mathrm{km\,s^{-1} Mpc^{-1}} \ , \\
k_f &= 2.94 \times 10^{-61}\,\mathrm{kg^{-1} s^{-1}} \ , \\
v_{flat} &= 135\,\mathrm{km\,s^{-1}} \ .
\end{aligned}
$$

The expansion parameter of the Milky Way H_r is now half its previous value. The frame constant k_f, which now applies to the system as a whole—with double the mass—also gets reduced by one half. In concert, Eq. (173) gives the significantly lower value for v_{flat} of 135 km s^{-1} in comparison to the value calculated above of 191 km s^{-1}. Interestingly, looking at v_{flat}, this two-galaxy system has a

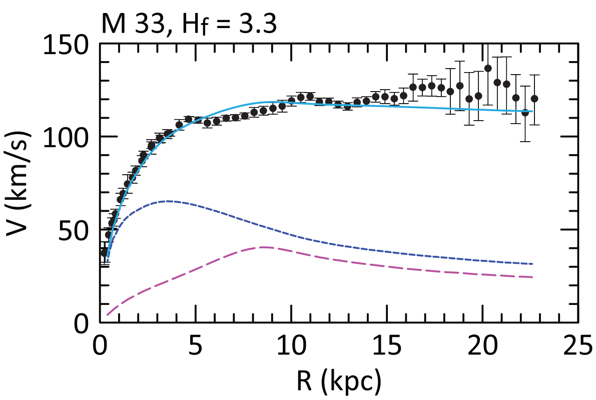

FIG. 11. The net rotation curve is drawn as a solid cyan line, and the Newtonian curves for the stellar and gas disks are drawn with dashed blue and magenta lines, respectively, with the magenta line having the larger dashes. Data are from Corbelli et al. 2014 [36].

significantly lower energy state—both in terms of kinetic and potential energies—than the case where the galaxies are independent. This is with all else being equal—including mass and peculiar speed.

The potential large disparity in energy states is an additional distinction in terms of what defines a system.

Based on Yoshiaki Sofue's work, it's possible that the Milky Way's rotation curve does flatten to 135 km s^{-1}. Recall that past 100 kpc, the error bars of Sofue's grand rotation curve allow for rotational velocities from 100 to 200 km s^{-1} [32]. With neither value for v_{flat}—135 or 191 km s^{-1}—ruled out, the question as to whether the Milky Way and Andromeda are part of a complete system remains unresolved. Clearly, an analysis of Andromeda's and the Milky Way's rotation curves would offer further evidence in a particular direction, but a look at Triangulum (M33) has the potential to be more informative.

The mass of M33 is an order of magnitude less than Andromeda (M31) (or the Milky Way) [35][36]. The implication is that if M33 is part of a system comprising one or both of its larger neighbors, its expansion parameter would be reduced by an order of magnitude in comparison to its value as an isolated galaxy. Further, the distance between M33 and M31 is estimated at 200-240 kpc [37], which opens the possibility that M33 could be a satellite of M31. An analysis of M33's rotation curve should provide a clear indication if this is indeed the case.

Fig. 11 shows M33's rotation curve, which was generated using the same finite-element method described above. Density profiles for the stellar disk and gas components were derived from Newtonian curves rendered by Corbelli et al. 2014 [36].

The net rotation curve was fit with the following values for m_t and H_f:

$$
\begin{aligned}
m_t &= 7.51 \times 10^9\,\mathrm{M}_\odot = 1.49 \times 10^{40}\,\mathrm{kg}\ , \\
H_f &= 3.3\,\mathrm{km\,s^{-1}Mpc^{-1}}\ , \\
v_f &= 666\,\mathrm{km\,s^{-1}}\ , \\
k_f &= 7.17 \times 10^{-60}\,\mathrm{kg^{-1}s^{-1}}\ , \\
v_{flat} &= 106\,\mathrm{km\,s^{-1}}\ .
\end{aligned}
$$

With these values for m_t and H_f, v_{flat} calculates to 106 km s^{-1}, which aligns with the figure.

The total mass m_t, gleaned via these density profiles, is in line with estimates from Corbelli's 2014 paper and a previous paper—Corbelli et al. 2003, which placed M33's mass at $5.4 - 8.4$E9 $M_\odot$ [35].

The expansion parameter H_f of 3.3 km s^{-1} Mpc^{-1} translates to a peculiar frame speed v_f of 666 km s^{-1}. This is not too far from the estimated peculiar speed of the Milky Way—at 565 km s^{-1}—and that of the Local Group—620 km s^{-1}. Two SPARC galaxies that are also considered part of the Local Group—NGC 3109 and UGCA 444—were estimated to have H_fs of 3.6 and 3.2 km s^{-1} Mpc^{-1}, respectively.

Notice that the frame constant k_f for M33 is an order of magnitude larger than that of the Milky Way. Given that M31 has a similar mass and peculiar speed to that of the Milky Way, M31's frame constant should also be an order of magnitude smaller than that of M33. As such, while M33 is certainly gravitationally influenced by M31—and likely gravitationally bound to M31—the two galaxies do not constitute a system—at least according to the present definition that all particles in the *complete* system share the same frame constant.

It's thus unlikely that M31 and the Milky Way are part of a larger complete system. Further, based on their expansion parameters—which range between 3.04 and 3.6 km s^{-1} Mpc^{-1}, each of the aforementioned galaxies in the Local Group (The Milky Way, M31, M33, NGC 3109, and UGCA 444) is seemingly independent of the others and does not likely constitute an element of a larger complete system.

Further investigation into the Local Group with the above questions in mind will be instructive. This should include an analysis of the rotation curves of M31 and the Milky Way, and the smaller pressure-supported galaxies, including the Globular Clusters on the outskirts of M31 and the Milky Way.

A large spiral galaxy such as the Milky Way has clearly absorbed and merged with other galaxies over the course of its history. How, dynamically, the expansion parameter evolves over time for the particles involved—as a galaxy with a certain frame constant merges with a second galaxy with a different frame constant—is also an important question to be explored.

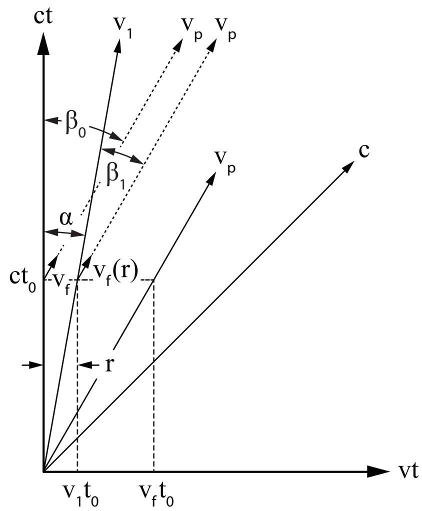

FIG. 12.

XVII. RELATIVE EXPANSION PARAMETER

If rotation curves can remain flat for hundreds of kpc, can they remain flat for hundreds of Mpc? Can they remain flat indefinitely? To address this question, building on the framework of Section XII, the concept of a "relative expansion parameter" $H_f(r)$—as an extension of the "frame expansion parameter" H_f—will be investigated with distance taken into account.

Fig. 12, similar to Fig. 9, is a spacetime diagram with a frame moving at speed v_p in the rest frame of a Hubble coordinate. Recall from Section XII that deceleration—as given by Eq. (164)—is calculated in the reference frame of the coincident coordinate—which is to say in the Hubble frame. In contrast to Fig. 9, the rest frame of Fig. 12 is that of the coincident coordinate, which is always the coordinate crossed by the moving frame at t_0—the current Hubble time in the rest frame. Notice that the moving frame is crossing the coordinate of the rest frame at t_0. At this moment, v_f is equivalent to v_p.

Recall that while v_f is measured relative to the coincident Hubble coordinate, v_p is measured relative to a fixed coordinate, or alternatively said, relative to an observer that is static in the Hubble frame. Thus, while v_p remains constant over time relative to this observer, v_f is always decreasing. Looking at the diagram, v_f decreases with distance as well. Notice that, at distance r in the rest frame, peculiar speed $v_f(r)$, which is measured relative to coincident coordinate v_1, is less than v_f—as shown by angle β_1—which is less than β_0. Here, peculiar speed $v_f(r)$ is defined as the peculiar speed at offset r in the rest frame.

As distance r in the rest frame increases, peculiar speed $v_f(r)$ decreases. At distance $v_f t_0$ from the ct axis, the slope of the coincident Hubble coordinate is equivalent to that of v_p. Across this distance—where the angle between v_p and the coincident coordinate is zero—a first observer in the frame at the ct axis would gauge that a second observer has a peculiar speed $v_f(r)$ of zero. Further, with the frame expansion parameter H_f being a function of v_f—as described by Eq. (164)—this first observer would also gauge that the second observer sees the frame as having an expansion parameter H_f of zero.

This raises a question: In previous sections, the expansion parameter of the parent frame H_f was deemed to be invariant with respect to motion and position—a value that was agreed upon by all particles in the system. Is this still the case? The answer is still yes. From the perspective of the first observer, the frame has an expansion parameter of H_f. Importantly, the second observer also agrees with this value and sees the frame as having the same expansion parameter of H_f. However, the first observer sees the second observer as existing in a frame with a smaller, relative expansion parameter of $H_f(r)$; and in congruence, the second observer sees the first as existing in the same relative frame—where each observer agrees on the value of other's relative expansion parameter $H_f(r)$.

Recognize that in the spacetime diagram of Fig. 12, there is no preferred observer in the moving frame. From the perspective of a first observer, a second observer at distance $v_f t_0$ has a peculiar speed $v_f(r)$ of zero. And likewise, from the perspective of the second observer, the first observer has a peculiar speed $v_f(r)$ of zero. Neither observer is preferred, and both agree that the other has a peculiar speed of zero. With Eq. (164), which relates peculiar speed to expansion parameter, each observer would see the other as existing in a frame with an expansion parameter of zero.

Further, because there is no preferred direction in the frame, two observers orthogonal to the first two—also at a distance of $v_f t_0$—would agree that the frame has an expansion parameter of zero as well, but only with respect to each other! If these four observers formed a square, a pair of neighboring observers would be closer than $v_f t_0$, in which case, each observer in this pair would see the other as having a non-zero expansion parameter.

As a practical matter, at the scale of the typical rotation curve, $H_f(r)$ does not deviate with any significance from H_f. However, at large scales—typically on the order of Mpc, $H_f(r)$ can be substantially lower than H_f.

To explore the relation between expansion parameter and distance, refer again to Fig. 12. Angles β_0 and β_1 in the diagram are related to speed as follows:

$$tan(\beta_0) = \frac{v_f}{c} \, , \tag{174}$$

$$tan(\beta_1) = \frac{v_f(r)}{c} \, . \tag{175}$$

Note that v_f in Eq. (174) is relative to the coincident Hubble coordinate of the rest frame; and $v_f(r)$—which is the peculiar speed at offset r—is relative to coincident coordinate v_1.

Similarly, a relation between distance r in the rest frame and angle α is as follows:

$$tan(\alpha) = \frac{r}{ct_0} \; . \tag{176}$$

Combining the equations above gives this:

$$\beta_1 = \beta_0 - \alpha \; , \tag{177}$$
$$tan(\beta_1) = tan(\beta_0 - \alpha) \; , \tag{178}$$
$$\frac{v_f(r)}{c} = tan\left(arctan\left(\frac{v_f}{c}\right) - arctan\left(\frac{r}{ct_0}\right)\right) \; , \tag{179}$$
$$\frac{v_f(r)}{c} = \left(\frac{v_f}{c} - \frac{r}{ct_0}\right)\left(1 + \left(\frac{v_f}{c}\right)\left(\frac{r}{ct_0}\right)\right)^{-1} \; , \tag{180}$$
$$v_f(r) = (v_f - rH_0)\left(1 + \frac{v_f r H_0}{c^2}\right)^{-1} \; . \tag{181}$$

Eq. (177) is derived with simple geometry. Imagine v_1 rotating counter-clockwise by α degrees about the origin in the diagram. This would bring v_1 in line with the ct axis—where β_1 would be equivalent to β_0.

Plugging Eqs. (174), (175), and (176) into Eq. (179), reduces to Eq. (180) via trigonometry and simplification. Plugging Eq. (118) into Eq. (180) gives Eq. (181).

Notice that, as r goes to zero in Eq. (181), $v_f(r)$ goes to v_f. This is as expected, as both speeds in this case would be relative to the same coincident coordinate. Thus, $v_f(0) = v_f$. As r goes to $v_f t_0$ (or alternatively, v_f/H_0), v_f goes to zero, which begs the question: What happens when r goes beyond $v_f t_0$? Can v_f go negative?

While velocity, which has direction, can be negative, it doesn't make physical sense for speed—which is the magnitude of velocity (which has no direction)—to be negative. This is consistent with Eq. (134)—where a non-negative peculiar speed v_f translates to deceleration in the Hubble frame. Looking at the spacetime diagram, all peculiar motion decelerates in the Hubble frame—including light, which asymptotically approaches the edge of the light cone.

Conversely, a negative v_f would result in positive acceleration in the Hubble frame, which, according to the diagram, could only happen with time running in reverse! Further, would a body perpetually accelerating in the Hubble frame—which is to say the observable universe—be guaranteed to stay within the universe? Is deceleration the universe's way of ensuring that no information can escape?

Additionally, looking at the relation for H_f given by Eq. (164), a negative v_f would result in H_f being imaginary and thus ill-defined. For these reasons, it's posited that v_f only has physical meaning as a non-negative value.

A relation for the expansion parameter $H_f(r)$—as seen by observers separated by distance r—is given by Eq. (164), where the peculiar speed in this equation is the value agreed upon by the observers—$v_f(r)$:

$$H_f(r) = \sqrt{\frac{v_f(r)}{c}} H_0 \; , \tag{182}$$
$$H_f(r)^2 = \frac{v_f(r)}{c} {H_0}^2 \; . \tag{183}$$

Plugging Eqs. (183) and (164) into Eq. (180) gives the following:

$$\frac{H_f(r)^2}{{H_0}^2} = \left(\frac{{H_f}^2}{{H_0}^2} - \frac{r}{ct_0}\right)\left(1 + \left(\frac{{H_f}^2}{{H_0}^2}\right)\left(\frac{r}{ct_0}\right)\right)^{-1} \tag{184}$$
$$H_f(r)^2 = \frac{({H_f}^2 - \frac{rH_0}{c}{H_0}^2){H_0}^2}{({H_0}^2 + \frac{rH_0}{c}{H_f}^2)} \; , \tag{185}$$
$$H_f(r) = H_0\sqrt{\frac{{H_f}^2 - \frac{rH_0}{c}{H_0}^2}{{H_0}^2 + \frac{rH_0}{c}{H_f}^2}} \; . \tag{186}$$

Hence, in a frame with peculiar speed v_f and expansion parameter H_f, Eq. (186) gives the relative expansion parameter $H_f(r)$ as a function of distance r. Notice that, similar to Eq. (181), as r goes to zero, $H_f(r)$ goes to the frame expansion parameter H_f. Thus, $H_f(0) = H_f$.

1. *Frame Extent x_0*

Here, a new parameter x_0, termed the "frame extent", is introduced that is defined as the distance where $H_f(r)$ goes to zero. The frame extent x_0 is derived via Eq. (186) as follows:

$${H_f}^2 - \frac{x_0 H_0}{c}{H_0}^2 = 0 \; ,$$
$$x_0 = \frac{c{H_f}^2}{{H_0}^3} \; . \tag{187}$$

Notice that, for light, which sees an expansion parameter of H_0, Eq. (187) reduces to Eq. (117)—where x_0 goes to r_0:

$$x_0 = \frac{c\cancel{{H_0}^2}}{H_0^{\cancel{3}}} \; ,$$
$$x_0 = r_0 = \frac{c}{H_0} \; .$$

Thus, the upper limit of the frame extent x_0 is the size of the observable universe r_0. The lower limit of x_0 is zero, which is seen with a frame expansion parameter H_f of zero.

Note that there is a difference between the frame extent x_0 and the frame size r_f: x_0 is an observable metric, whereas r_f is conceptual. With Eqs. (159) and (117), restated below, r_f relates to x_0 as follows:

$$
\begin{aligned}
r_f &= r_0\frac{H_f}{H_0}\ , \\
r_0 &= \frac{c}{H_0}\ , \\
r_f &= \frac{cH_f}{{H_0}^2}\ , \\
r_f\frac{H_f}{H_0} &= \frac{c{H_f}^2}{{H_0}^3} = x_0\ , \\
r_f H_f &= x_0 H_0\ . \qquad (188)
\end{aligned}
$$

Looking at Eq. (188), with H_f being less than or equal to H_0, the frame extent x_0 must be less than or equal to the frame size r_f. As H_f goes to H_0, r_f goes to x_0; and as H_f goes to H_0, both r_f and x_0 go to r_0. As H_f goes to zero—looking at Eqs. (159) and (188)—both r_f and x_0 go to zero.

With Eq. (160), Eq. (188) further equates to:

$$
r_f H_f = x_0 H_0 = v_f\ . \qquad (189)
$$

Thus, in relation to r_f, x_0 is the distance in the Hubble frame where the rate of expansion v_f is equivalent to the rate of expansion of the moving frame at r_f. Keep in mind that v_f is also the peculiar speed of the moving frame in the Hubble frame.

2. *Relative Frame Constant $k_f(r)$*

If measuring the expansion parameter of the parent frame across a distance can result in a relative value described by $H_f(r)$ that deviates from H_f, where does this leave frame constant k_f?

Recall from Section X that the positions and motions of the particles comprising a system have no bearing on the expansion parameter of the frame containing the system. The expansion parameter is a property of the frame alone.

This is still the case in the present situation. Further, it is still true that all particles in the complete system have the same frame constant k_f, which is defined by Eq. (168) as the expansion parameter per unit mass. Thus k_f may still be calculated by dividing the frame expansion parameter H_f by the total system mass m_t.

The frame expansion parameter H_f remains in effect and is distributed across all particles in the complete system. In relation to the peculiar speed of the frame, any point in the frame could be considered as the instantaneous "origin"—where $v_f(r) = v_f(0) = v_f$. Thus, any single point would see the frame having an expansion parameter of $H_f(r) = H_f(0) = H_f$. Because every particle in the system agrees on the frame's expansion parameter, it can be imagined that they all have the same state—which is to say the same frame constant k_f.

However, while particles *in isolation* have the same frame constant k_f, akin to $H_f(r)$, a first particle will see a second particle in the system—at a distance r—as having a smaller, relative frame constant $k_f(r)$. Reciprocally, the second particle will see the first particle as having this same relative frame constant—$k_f(r)$. Building on Eq. (168), a relation for $k_f(r)$ is as follows:

$$
\begin{aligned}
k_f(r) &= \frac{H_i(r)}{m_i} = \frac{H_f(r)}{m_t}\ , \qquad (190) \\
k_c(r) &= \frac{2\sqrt{ck_f(r)}}{\sqrt{G}} = \frac{2\sqrt{cH_f(r)}}{\sqrt{m_t G}}\ , \qquad (191) \\
a_n &= \frac{m_r G}{r}\left(\frac{1}{r} + k_c(r)\right)\ . \qquad (192)
\end{aligned}
$$

Consolidating the constants of the expansion component into one parameter gives the relative "system constant" $k_c(r)$ as defined by Eq. (191). Eq. (192) gives the simplified equation for acceleration a_n using $k_c(r)$.

If the relative expansion parameter $H_f(r)$ varies with distance—with one particle seeing another as existing in a relative frame that varies with distance—is it possible that $H_f(r)$ also varies with time and speed?

Looking at Eq. (164), H_f is already a function of time and speed—H_0 and v_f. Recall that H_0 is defined as the inverse of the Hubble time t_0 and thus, by definition, changes with time—asymptotically approaching zero. v_f is the peculiar speed relative to the Hubble frame and asymptotically approaches zero as well. Recall that inertial frames with non-zero peculiar speeds are always decelerating in the Hubble frame.

Thus, the expansion parameter H_f of a moving frame decreases over time—asymptotically approaching zero. It's not unreasonable, then, to imagine that the expansion parameter would decrease over distance as well—as described by relative expansion parameter $H_f(r)$. **Importantly, like H_f, $H_f(r)$ is a property of the frame and not its contents.**

Again, particles in isolation will all still measure the parent frame as having an expansion parameter of H_f—regardless of their positions and velocities relative to the frame. It's only when two particles, separated by a distance, measure the frame in unison that they see a relative value $H_f(r)$, which differs from the frame parameter H_f. Therefore, the frame's relative expansion parameter weakens with time *and* distance. Hence, measuring the frame at different times and across varying distances will give disparate results.

Note that while H_f *will* diminish over time, the rate of change of H_0 and v_f in Eq. (164) is negligible—as evidenced by $\dot{H}_0$ in Eq. (120), which calculates to an extremely small rate. To put this number in perspective: In another 13.8 billion years—the estimated age of the universe—the Hubble parameter will not have quite dropped from 70 to 69 km s^{-1} Mpc^{-1}.

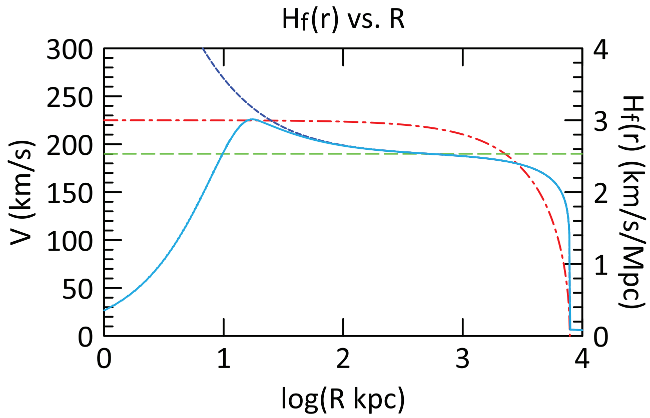

FIG. 13. A simulated galaxy with only a bulge. The net rotation curve is drawn as a solid cyan line. The blue line with small dashes is the rotation curve with the galaxy mass concentrated at a point. The green dashed line plots v_{flat}, and the red dash-dot line plots $H_f(r)$ vs. distance.

3. *A 10-Mpc Rotation Curve*

Fig. 13 shows the rotation curve of a simulated galaxy that extends out to 10 Mpc. The curve was generated identically to the other curves herein—via Eq. (70)—but with H_f in this equation having been replaced by $H_f(r)$—as given by Eq. (186).

The cyan line in Fig. 13 plots the curve for a galaxy with only a bulge—no stellar and gas disks. The blue line with small dashes plots the curve for the case where the equivalent galaxy mass is concentrated at a point. The parameters for this galaxy are nearly identical to those of the Milky Way:

$$\begin{aligned} m_t &= 1.67 \times 10^{41}\,\mathrm{kg}\ , \\ H_f &= 3.0\,\mathrm{km\,s^{-1}Mpc^{-1}}\ , \\ v_{flat} &= 190\,\mathrm{km\,s^{-1}}\ , \\ x_0 &= 7.87\,\mathrm{Mpc}\ . \end{aligned}$$

The red dash-dot line plots $H_f(r)$ vs. distance. Notice that $H_f(r)$ remains substantially flat out to 1 Mpc—where it has only dropped from 3.0 to 2.8 km s^{-1} Mpc^{-1}. From 1 to 6 Mpc, $H_f(r)$ declines nearly linearly to 1.5 km s^{-1} Mpc^{-1}. Beyond 6 Mpc, there is a rapid decline to zero at 7.87 Mpc, which is the value of frame extent x_0 for the parent frame—as calculated via Eq. (186). At this distance and beyond, $H_f(r)$ is zero, and the gravitational acceleration between particles in the frame is purely Newtonian.

The green dashed line plots v_{flat} for the galaxy, which calculates to 190 km s^{-1}. The rotation curve is nearly flat from 100 kpc to 2.8 Mpc. At 100 kpc, the rotational velocity is 5% above v_{flat} (at around 200 km/s). By 2.8 Mpc, the velocity has fallen to 5% below v_{flat} (at roughly 180 km/s), which constitutes a slope of -7.4 km s^{-1} Mpc^{-1}.

Referring back to the isolated galaxies with rotation curves that remain substantially flat out to 1 Mpc published by Mistele et al. [17], it's predicted that, if the technology existed to look beyond 1 Mpc, these curves would eventually show declines similar to the curve of Fig. 13. Further, it's predicted that there's a distance—the frame extent x_0—for each curve where the rotational velocity effectively drops to zero.

If the galaxies of the Local Group are bound within the frame extents of the three main galaxies—at roughly 8 Mpc, it's reasonable to imagine that this is the case for other galaxy groups and clusters. When thinking about larger structures, it's not necessary that every galaxy reside within the frame extent of every other galaxy. In other words, galaxies or groups can be chained together, where only the frame extents of individual links (or series of links) overlap. Extrapolating further, is it possible that the large-scale structures we observe in the universe—such as filaments and walls—are the result of such chaining—a phenomenon that allows these structures to form and remain stable over billions of years?

In summary, the expansion component of acceleration does not extend indefinitely but has a specific reach, and only within this range does it make a meaningful contribution to the motions of bodies. In relatively small galactic subsystems such as our Solar System, its effect is negligible. It does not measurably contribute to the motions of bodies. Even out to 10 light-years, the expansion component is so small relative to the Newtonian component—orders of magnitude less—that it can safely be ignored. However, in the range of kpc to Mpc, the expansion component can become significant and eventually dominant. But as frame extent x_0 is approached, this component rapidly drops to zero.

Upon reflection, the expansion component of acceleration *must* have a limited range. If rotation curves remained flat indefinitely, then the accelerating fields underpinning those curves would have to extend indefinitely as well. Were this the case, the pull between bodies across vast distances would be far too large for the universe to have the structure and dynamics we observe.

XVIII. DYNAMIC MASS

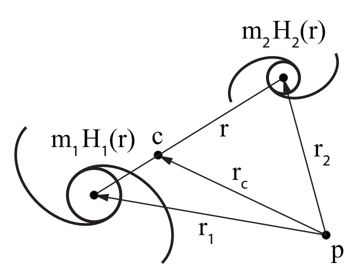

FIG. 14.

While the range of the expansion component is finite, it can still extend far enough to affect nearby galaxies.

For example, the simulated galaxy of Section XVII with the frame expansion parameter H_f of 3 km s^{-1} Mpc^{-1} has a frame extent x_0 of 7.87 Mpc, which encompasses most, if not all, of the galaxies in the Local Group. It's not unreasonable to imagine that 3 km s^{-1} Mpc^{-1} might be near the average expansion parameter for galaxies. Recall that the Milky Way has an estimated H_f of 3.04 km s^{-1} Mpc^{-1}; and as shown in Fig. 10, an H_f of 3.09 km s^{-1} Mpc^{-1} corresponds to the MOND constant a_0, which has been checked against a large catalog of galaxies.

In Section XVI, it was reasoned that the main galaxies of the Local Group—the Milky Way, M31, and M33, taken in any combination, are not part of a larger complete system as defined in the section. Yet, they are gravitationally bound—with each having a frame extent of roughly 8 Mpc—corresponding to a frame expansion parameter of nearly 3 km s^{-1} Mpc^{-1}.

To explore how these galaxies influence each other, refer to Fig. 14, which shows two galaxies—each comprising a complete system—of different mass, expansion parameter, and frame constant. Recall that all particles in the complete system, by definition, must have the same frame constant k_f—as well as the system constant k_c. Here, galaxies one and two have system constants k_{c1} and k_{c2}, respectively, that are not equivalent.

The acceleration with respect to galaxy one at distance r is given by Eq. (192):

$$a_1 = \frac{m_1 G}{r}\left(\frac{1}{r} + k_{c1}(r)\right) . \tag{193}$$

Here, it's assumed that galaxies one and two are sufficiently far apart that they may be considered point masses.

Similarly, the acceleration with respect to galaxy two at distance r is thus:

$$a_2 = \frac{m_2 G}{r}\left(\frac{1}{r} + k_{c2}(r)\right) . \tag{194}$$

Looking at Eqs. (193) and (194), the following inequality is apparent:

$$m_2 a_1 \neq m_1 a_2 .$$

Here, it's presumed that particles external to a system see the same acceleration as particles within the system. The particles of galaxy two experience an acceleration a_1 toward galaxy one and likewise, the particles of galaxy one experience an acceleration a_2 toward galaxy two.

Thus, referring to Fig. 14, a distant, isolated inertial observer at point p would not see point c—the barycenter of galaxies one and two—maintaining constant velocity over time:

$$\frac{d^2}{(dt)^2}\vec{r}_c \neq 0 .$$

This is problematic because this equation indicates that conservation of momentum in the Newtonian limit is being violated.

There is, however, a "dynamic mass" $m_1{}'$ and a dynamic mass $m_2{}'$ such that the following equation is satisfied:

$$m_2{}' a_1 = m_1{}' a_2 . \tag{195}$$

With Eq. (195), relations for $m_1{}'$ and $m_2{}'$ are as follows:

$$\begin{aligned}
\frac{m_1{}'}{m_2{}'} &= \frac{a_1}{a_2} , \\
\frac{m_1{}'}{m_2{}'} &= \frac{\frac{m_1 G}{r}\left(\frac{1}{r} + k_{c1}(r)\right)}{\frac{m_2 G}{r}\left(\frac{1}{r} + k_{c2}(r)\right)} , \\
\frac{m_1{}'}{m_2{}'} &= \frac{m_1\left(1 + r k_{c1}(r)\right)}{m_2\left(1 + r k_{c2}(r)\right)} , \\
m_1{}' &= m_1\left(1 + r k_{c1}(r)\right) , & (196)\\
m_2{}' &= m_2\left(1 + r k_{c2}(r)\right) . & (197)
\end{aligned}$$

Looking at Eqs. (196) and (197), a general relation for dynamic mass m' as a function of ordinary mass m and relative system constant $k_c(r)$ is as follows:

$$m' = m\left(1 + r k_c(r)\right) . \tag{198}$$

Looking at Eq. (198), the dynamic mass m' has two components—the ordinary-mass term m and the dynamic term $r k_c(r)$, which, for a given complete system, is purely a function of distance r.

Notice that the $1/r$ expansion component of acceleration is recovered when dynamic mass m' is plugged into Newton's Law of Gravitation. Thus, it's imagined that a plot of the dynamic term in Eq. (198)—for the typical rotationally-supported galaxy with a flat rotation curve—would look very similar to the typical hypothesized dark-matter halo. Keep in mind that $k_c(r)$ goes to zero as the frame extent x_0 is approached, so the dynamic-mass halo is always finite in size.

The expansion-acceleration component a_e of net acceleration a_n in Eq. (192) is as follows:

$$a_e = \frac{m_r G k_c(r)}{r} . \tag{199}$$

Recall from Section I that, vectorially, acceleration is opposite the direction of information flow. At distances where $(r \ll x_0)$, $k_c(r)$ can be considered constant. In this range, a_e simplifies to:

$$a_e = \frac{m_r G k_c}{r} = \frac{k}{r} . \tag{200}$$

Here, a_e is a measure of the strength of a vector field propagating radially outward from source mass m_r—where, in response to this field, there is an acceleration a_e pointed towards the source. The divergence of this vector field in polar coordinates is as follows:

$$div\ a_e = \nabla \cdot a_e = \frac{1}{r^2}\frac{\partial}{\partial r}\left(r^2\frac{k}{r}\right) \ ,$$
$$div\ a_e = \frac{k}{r^2} \ .$$

The positive divergence of a_e indicates that points in the field are sources of the field. Because this is a gravitational field, its source is mass/energy, which is to say points in the a_e field are sources of energy. This aligns with the premise of Section IV, which describes the expansion component of acceleration as deriving from the interaction between expanding space and points in a Newtonian gravitational field.

Because the energy of the a_e field is coupled with time uncertainty, it's speculated that the energy in this field is borrowed from the vacuum. This aligns with the connection between expanding space and energy broached in Section XIII via Eqs. (156) and (144). Eq. (156) indicates that, as the observable universe expands at c, its net energy continually increases at the Planck power. Eq. (144) maintains that the time uncertainty Δt_u of the observable universe is *always* double the Hubble time t_0, which—because the net energy of the observable universe directly derives from Δt_u—implies that this energy is perpetually on loan.

Interestingly, flat galactic rotation curves seem to be a result of two phenomena that are simultaneously true. One, Newtonian gravity interacting with expanding space results in the manifestation of a second $1/r$ acceleration component (the expansion component a_e) on top of the Newtonian component. At the same time, the field that comprises the expansion component has dynamic mass that is distributed such that its gravitational field (which is Newtonian) yields the same acceleration at the same points in space as the $1/r$ component.

Similarly, the presence of this $1/r$ field increases the momentum of the galaxy by the amount of dynamic mass in the field. Hence, in the end, it's concluded that the "missing mass"—the "dark matter"—in galaxies is a $1/r$ field that is generated as a result of expanding space.

Eq. (195)—as applied to two bodies *within* and part of the complete system having a system constant of k_c—resolves as follows:

$$m_2{}'a_1 = m_1{}'a_2 \ ,$$
$$m_2\cancel{(1+rk_c(r))}\,a_1 = m_1\cancel{(1+rk_c(r))}\,a_2 \ ,$$
$$m_2a_1 = m_1a_2 \ .$$

Bodies within a system all see the same frame constant k_f and thus the same system constant k_c. Two bodies separated by distance r, in unison, see the frame as having a relative system constant of $k_c(r)$, and both agree on its value. Thus, the dynamic terms of $m_1{}'$ and $m_2{}'$ cancel, and Eq. (195) reduces to the familiar Third Law of Motion—with non-dynamic mass terms.

If, however, $m_1{}'$ and $m_2{}'$ represent bodies or particles in separate systems with different relative system constants $k_{c1}(r)$ and $k_{c2}(r)$, the dynamic terms of these masses do not cancel:

$$m_2{}'a_1 = m_1{}'a_2 \ ,$$
$$m_2\left(1+rk_{c2}(r)\right)a_1 = m_1\left(1+rk_{c1}(r)\right)a_2 \ .$$

Expanding the a_1 and a_2 terms, gives this:

$$\frac{m_1m_2G}{r^2}\left(1+rk_{c2}(r)\right)\left(1+rk_{c1}(r)\right) =$$
$$\frac{m_1m_2G}{r^2}\left(1+rk_{c1}(r)\right)\left(1+rk_{c2}(r)\right) \ .$$

Notice that, beyond the frame extents of m_1 and m_2—where $k_{c1}(r)$ and $rk_{c2}(r)$ go to zero, the above equation resolves to the familiar relation for Newtonian gravity.

1. General Relativity

Any modification to gravity should ultimately have a generally covariant formulation. General covariance is the understanding that physical laws are independent of the specific coordinate system in which they are described. General relativity is a generally covariant theory that describes gravity as the curvature of spacetime, with that curvature related to the stress-energy tensor through Einstein's field equations. As general relativity has passed nearly every test thrown at it, any modification to gravity must reduce to general relativity—as it's currently understood—in contexts where general relativity has been verified to high precision, such as the Solar System.

The word "nearly" in the above paragraph relates to the flat rotation curves of galaxies, which, according to general relativity, necessitate the presence of dark matter—typically in the form of a massive halo. Flat rotation curves are generated via Eq. (70) with no need for dark matter. Ironically, however, this same equation—when viewed from another angle—can be construed as the source of dynamic mass—that, when plotted against the backdrop of the typical galaxy with a flat rotation curve—looks a lot like a dark-matter halo!

Thus, it's estimated that the proposed modification to gravity may be incorporated into general relativity without altering Einstein's field equations, provided that the effective dynamic mass can be consistently represented within the stress-energy tensor. A relativistic formulation of this stress-energy tensor is left for future work.

Further, because this framework only requires a modification to the stress-energy tensor, the pitfalls of TeVeS (Tensor-Vector-Scalar)—which is a relativistic formulation for MOND—are potentially avoided. TeVeS predicted that gravitational waves from GW170817 should have arrived approximately 400 days out of sync with the light signal from the merger of binary stars GW170817 and GRB 170817A, which was not the case [38]. The authors of the cited paper note that not all modified gravity models are necessarily falsified by the data. It's estimated that the present model allows for transverse gravitational waves that travel at c, but this will have to be confirmed in the forthcoming paper.

XIX. SUMMARY

The core concept of the paper is embodied by Eq. (21), which relates acceleration $\vec{a}$ in a field to the speed of information in the field c and time uncertainty Δt_u—the latter a measure of how efficiently that information can be transmitted to a particle in the field:

$$\vec{a} = -\frac{2\vec{c}}{\Delta t_u} \; .$$

Note that $\vec{a}$—which is opposite the direction of information flow c—in Eq. (21) is a measure of the field strength that only translates to the kinematic acceleration of a particle in the field—in the Newtonian limit.

Eq. (21) was derived via the uncertainty principle as applied to Newtonian gravity. The relation was also used to recover the Coulomb force between two electrons. With this in mind, it's imagined that Δt_u could refer to the lifespan of a virtual graviton.

Eq. (21) was also used to calculate the mass of the observable universe—as given by Eq. (153):

$$m_0 = \frac{c^3}{GH_0} = \frac{c^3 t_0}{G} \; .$$

At the current Hubble time t_0, the mass of the observable universe m_0 calculates to 1.78E53 kg.

In Section XII, it is shown that a frame with a non-zero peculiar speed relative to the Hubble frame is decelerating in the Hubble frame. This deceleration is proportional to peculiar speed v_f—as given by Eq. (134):

$$a_f = -v_f H_0 \; .$$

It's presumed that this deceleration has physical effects. As v_f goes to zero, deceleration a_f goes to zero—where these physical effects disappear.

For light, deceleration a_f is maximized—as described Eq. (135):

$$a_f = -cH_0 \; .$$

The observed effect on light—as it decelerates—is redshift. Interestingly, redshift can be explained in two contexts: the wavelength of a photon being stretched over time *or* a photon losing energy as it travels in a decelerating field. Combining Eqs. (135) and Eq. (21) ultimately reduces to Eq. (153)—the relation for the mass of observable universe m_0.

Because any point in space can be the origin of expansion, it's imagined that any frame moving in the Hubble frame can have its own origin of expansion—with the moving frame having an expansion parameter of H_f. A general relation for the expansion parameter H_f of a frame with a peculiar speed of v_f is given by Eq. (164):

$$H_f = \sqrt{\frac{v_f}{c}} H_0 \; .$$

Notice that, as v_f goes zero, H_f goes to zero and as v_f goes to c, H_f goes to H_0. Thus, a frame traveling at c sees the full expansion parameter of the parent frame—H_0.

It's posited that gravitational fields are also subject to being redshifted. It's imagined that the redshift of a Newtonian field yields a second $1/r$ field. Particles in this field experience an additional acceleration component termed the "expansion component". This and the Newtonian component are embodied in Eq. (70), which gives the net acceleration a_n relative to a reference mass m_r at distance r—in the Newtonian limit:

$$a_n = \frac{m_r G}{r} \left(\frac{1}{r} + \frac{2\sqrt{cH_f}}{\sqrt{m_t G}} \right) \; .$$

Here, m_t is the mass of a system with an expansion parameter H_f—the latter a function of the system's peculiar speed v_f as described by Eq. (164). When applied to galaxies, this equation produces flat rotation curves in agreement with observations.

The mechanism for the expansion component is thus: While the redshift of light progresses over time, the strength of a gravitational field, as a function of the source mass, remains invariant—assuming a constant mass. Thus, as a gravitational field is redshifted, it is continuously re-informed by the source mass. The tension between redshift and re-information can be measured by time uncertainty Δt_u, which—via Eq. (21)—yields the additional acceleration term in Eq. (70). As before, Δt_u could imply the existence of a virtual graviton—where this tension manifests as gravitons that amplify the existing field.

1. *Predictions*

The present thesis makes two notable predictions: One, because expansion parameter H_f is a function of peculiar speed, it's predicted that galaxies may be found with rotation curves with some measure of decline that will lie somewhere between flat and Keplerian. However, as most galaxies and groups are estimated to be part of a bulk mass flow, the probability of finding a galaxy with a peculiar speed near zero seems low. Further, because there is not a precise way to measure the transverse velocity of a distant galaxy, it will be difficult to verify that galaxy's true peculiar speed.

Two, Eq. (186) places a limit x_0 on the extent of a flat rotation curve as follows:

$$x_0 = \frac{cH_f{}^2}{H_0{}^3} \ .$$

This prediction is also difficult to test. For example, the frame extent x_0 of the Milky Way is estimated at 7.87 Mpc. An isolated galaxy with a flat rotation curve would have to be identified, and then its rotation curve would have to be measured out to several Mpc, which is not a trivial undertaking.

The forthcoming relativistic analysis of this thesis may offer the best avenue for falsification—as one prediction may be that gravitational waves traveling through a galaxy with the proposed $1/r$ field would be polarized.

---

[1] F. Shu, *The Physical Universe: An Introduction to Astronomy*, G - Reference,Information and Interdisciplinary Subjects Series (University Science Books, 1982).

[2] Wikipedia contributors, Observable universe — Wikipedia, the free encyclopedia (2026), [Online; accessed 31-May-2026].

[3] N. Aghanim *et al.*, Planck 2018 results: Vi. cosmological parameters, Astronomy & Astrophysics **641**, A6 (2020).

[4] A. Zee, *Quantum Field Theory in a Nutshell*, 2nd ed. (Princeton University Press, 2010).

[5] M. Milgrom, A modification of the newtonian dynamics as a possible alternative to the hidden mass hypothesis, Astrophysical Journal, Letters **270**, 365 (1983).

[6] M. Milgrom, A modification of the newtonian dynamics - implications for galaxies, Astrophysical Journal, Letters **270**, 371–389 (1983).

[7] M. Milgrom, A modification of the newtonian dynamics - implications for galaxy systems, Astrophysical Journal, Letters **270**, 384 (1983).

[8] K. G. Begeman, A. H. Broeils, and R. H. Sanders, Extended rotation curves of spiral galaxies : dark haloes and modified dynamics., mnras **249**, 523 (1991).

[9] R. B. Tully and J. R. Fisher, A new method of determining distances to galaxies, Astronomy and Astrophysics **54**, 661–673 (1977).

[10] S. S. McGaugh, J. M. Schombert, G. D. Bothun, and W. J. G. de Blok, The baryonic tully-fisher relation, The Astrophysical Journal **533**, L99 (2000).

[11] S. S. McGaugh, The baryonic tully-fisher relation of galaxies with extended rotation curves and the stellar mass of rotating galaxies, The Astrophysical Journal **632**, 859 (2005).

[12] S. S. McGaugh and W. J. G. de Blok, Testing the hypothesis of modified dynamics with low surface brightness galaxies and other evidence, Astrophysical Journal, Letters **499**, 66 (1998).

[13] R. H. Sanders, Modified newtonian dynamics: A falsification of cold darkmatter, Advances in Astronomy (2009), 752439.

[14] S. S. McGaugh, Novel test of modified newtonian dynamics with gas rich galaxies, Physical Review Letters **106** (2011), 121303.

[15] S. S. McGaugh, The baryonic tully-fisher relation of gas-rich galaxies as a test of λcdm and mond, Astronomical Journal **143** (2012), 40.

[16] F. Lelli, S. S. McGaugh, and J. M. Schombert, The small scatter of the baryonic tully–fisher relation, The Astrophysical Journal Letters **816**, L14 (2016).

[17] T. Mistele, S. McGaugh, F. Lelli, J. Schombert, and P. Li, Indefinitely flat circular velocities and the baryonic tully–fisher relation from weak lensing, The Astrophysical Journal Letters **969**, L3 (2024).

[18] S. S. McGaugh, Testing galaxy formation and dark matter with low surface brightness galaxies, Studies in History and Philosophy of Science **88**, 220 (2021).

[19] Sneppen, Albert, Watson, Darach, Poznanski, Dovi, Just, Oliver, Bauswein, Andreas, and Wojtak, Radosław, Measuring the hubble constant with kilonovae using the expanding photosphere method, A&A **678**, A14 (2023).

[20] D. Brout, Scolnic, *et al.*, The pantheon+ analysis: Cosmological constraints, The Astrophysical Journal **938**, 110 (2022).

[21] E. P. Tryon, Is the universe a vacuum fluctuation?, Nature **246**, 396 (1973).

[22] J. C. Carvalho, Derivation of the mass of the observable universe, International Journal of Theoretical Physics **34**, 2507 (1995).

[23] C. Mercier, Calculation of the mass of the universe, the radius of the universe, the age of the universe and the quantum of speed., Journal of Modern Physics **10**, 980 (2019).

[24] S. Weinberg, *Gravitation and Cosmology* (John Wiley & Sons, 1972).

[25] P. Li, F. Lelli, S. McGaugh, and J. Schombert, A comprehensive catalog of dark matter halo models for sparc galaxies, The Astrophysical Journal Supplement Series **247**, 31 (2020).

[26] M. W. Weinberg, Analysis of the sparc galactic catalog with modified gravity, https://github.com/mweinberg8721/modified-gravity-simulator.

[27] NASA/IPAC Extragalactic Database, The NASA/IPAC Extragalactic Database (NED) is operated by the Jet Propulsion Laboratory, California Institute of Technology, under contract with the National Aeronautics and Space Administration., https://ned.ipac.caltech.edu/.

[28] Hagala, R., Llinares, C., and Mota, D. F., The slingshot effect as a probe of transverse motions of galaxies, A&A **628**, A30 (2019).

[29] J. Klačka, M. Šturc, and E. Puha, Milky Way: New Galactic mass model for orbit computations, arXiv e-prints , arXiv:2407.12551 (2024), arXiv:2407.12551 [astro-ph.GA].

[30] A.-C. Eilers, D. W. Hogg, H.-W. Rix, and M. K. Ness, The circular velocity curve of the milky way from 5 to 25 kpc, The Astrophysical Journal **871**, 120 (2019).

[31] H.-F. Wang, Z. Chrobáková, M. López-Corredoira, and F. Sylos Labini, Mapping the milky way disk with gaia dr3: 3d extended kinematic maps and rotation curve to ≈30 kpc, The Astrophysical Journal **942**, 12 (2022).

[32] Y. Sofue, Dark halos of m31 and the milky way, Publications of the Astronomical Society of Japan

67, 75 (2015), https://academic.oup.com/pasj/article-pdf/67/4/75/54682398/pasj_67_4_75.pdf.

[33] R. S. Park, W. M. Folkner, A. S. Konopliv, J. G. Williams, D. E. Smith, and M. T. Zuber, Precession of mercury's perihelion from ranging to the messenger spacecraft, The Astronomical Journal **153**, 121 (2017).

[34] P. R. Kafle, S. Sharma, G. F. Lewis, A. S. G. Robotham, and S. P. Driver, The need for speed: escape velocity and dynamical mass measurements of the andromeda galaxy, Monthly Notices of the Royal Astronomical Society **475**, 4043 (2018), https://academic.oup.com/mnras/article-pdf/475/3/4043/23934699/sty082.pdf.

[35] E. Corbelli, Dark matter and visible baryons in m33, Monthly Notices of the Royal Astronomical Society **342**, 199 (2003), https://academic.oup.com/mnras/article-pdf/342/1/199/3574568/342-1-199.pdf.

[36] Corbelli, Edvige, Thilker, David, Zibetti, Stefano, Giovanardi, Carlo, and Salucci, Paolo, Dynamical signatures of a λcdm-halo and the distribution of the baryons in m33, A&A **572**, A23 (2014).

[37] A. Sarajedini, A differential rr lyrae line-of-sight distance between m31 and m33, Monthly Notices of the Royal Astronomical Society **508**, 3035 (2021).

[38] S. Boran, S. Desai, E. O. Kahya, and R. P. Woodard, Gw170817 falsifies dark matter emulators, Phys. Rev. D **97**, 041501(R) (2018).